of GATA-6 on SULT2A1 reporter gene activity was additive with MED1. These results indicate that the expression of SULT2A1 is controlled by not only transcription factors but also their coactivators. Our findings suggest that further studies are needed to define the role of other candidate coactivators in the expression of SULT2A1 and other genes involved in adrenal androgen biosynthesis.

In summary, we confirmed the expression of MED1 mRNA and protein in the adrenal gland and demonstrated that MED1 additively enhanced GATA-6 activation of CYP11A1, CYP17, and SULT2A1 promoter constructs. Down-regulation of MED1 also decreased DHEAS biosynthesis. These data support the hypothesis that adrenal DHEAS production can be regulated by GATA-6 and MED1.

Acknowledgments

Address all correspondence and requests for reprints to: William E. Rainey, Ph.D., Department of Physiology, Medical College of Georgia, 1120 15th Street, CA-3094, Augusta, Georgia 30912. E-mail: wrainey@mcg.edu.

This work was supported by Grants DK69950, DK43140, and HD11149 from the National Institutes of Health (to W.E.R.).

Disclosure Summary: W.E.R. was supported by the National Institutes of Health. Other authors have nothing to declare.

References

1. Rainey WE, Carr BR, Sasano H, Suzuki T, Mason JI 2002 Dissecting human adrenal androgen production. Trends Endocrinol Metab 13: 234–239
2. Kennerson AR, McDonald DA, Adams JB 1983 Dehydroepiandrosterone sulfotransferase localization in human adrenal glands: a light and electron microscopic study. J Clin Endocrinol Metab 56: 786–790
3. Suzuki T, Sasano H, Takeyama J, Kaneko C, Freije WA, Carr BR, Rainey WE 2000 Developmental changes in steroidogenic enzymes in human postnatal adrenal cortex: immunohistochemical studies. Clin Endocrinol (Oxf) 53:739–747
4. Saner KJ, Suzuki T, Sasano H, Pizzey J, Ho C, Strauss JF, Carr BR, Rainey WE 2005 Steroid sulfotransferase 2A1 gene transcription is regulated by steroidogenic factor 1 and GATA-6 in the human adrenal. Mol Endocrinol 19:184–197
5. Seely J, Amigh KS, Suzuki T, Mayhew B, Sasano H, Giguere V, Laganière J, Carr BR, Rainey WE 2005 Transcriptional regulation of dehydroepiandrosterone sulfotransferase (SULT2A1) by estrogen-related receptor α. Endocrinology 146:3605–3613
6. Crawford SE, Qi C, Misra P, Stellmach V, Rao MS, Engel JD, Zhu Y, Reddy JK 2002 Defects of the heart, eye, and megakaryocytes in peroxisome proliferator activator receptor-binding protein (PBP) null embryos implicate GATA family of transcription factors. J Biol Chem 277:3585–3592
7. Zhu Y, Qi C, Jain S, Rao MS, Reddy JK 1997 Isolation and characterization of PBP, a protein that interacts with peroxisome proliferator-activated receptor. J Biol Chem 272:25500–25506
8. Zhu Y, Qi C, Jain S, Le Beau MM, Espinosa 3rd R, Atkins GB, Lazar MA, Yeldandi AV, Rao MS, Reddy JK 1999 Amplification and overexpression of peroxisome proliferator-activated receptor binding protein (PBP/MED1) gene in breast cancer. Proc Natl Acad Sci USA 96:10848–10853
9. Yuan CX, Ito M, Fondell JD, Fu ZY, Roeder RG 1998 The TRAP220 component of a thyroid hormone receptor-associated protein (TRAP) coactivator complex interacts directly with nuclear receptors in a ligand-dependent fashion. Proc Natl Acad Sci USA 95:7939–7944
10. Rachez C, Lemon BD, Suldan Z, Bromleigh V, Gamble M, Näär AM, Erdjument-Bromage H, Tempst P, Freedman LP 1999 Ligand-dependent transcription activation by nuclear receptors requires the DRIP complex. Nature 398:824–828
11. Näär AM, Beaurang PA, Zhou S, Abraham S, Solomon W, Tjian R 1999 Composite co-activator ARC mediates chromatin-directed transcriptional activation. Nature 398:828–832
12. Kiiveri S, Liu J, Westerholm-Ormio M, Narita N, Wilson DB, Voutilainen R, Heikinheimo M 2002 Differential expression of GATA-4 and GATA-6 in fetal and adult mouse and human adrenal tissue. Endocrinology 143:3136–3143
13. Jimenez P, Saner K, Mayhew B, Rainey WE 2003 GATA-6 is expressed in the human adrenal and regulates transcription of genes required for adrenal androgen biosynthesis. Endocrinology 144:4285–4288
14. Kiiveri S, Liu J, Heikkilä P, Arola J, Lehtonen E, Voutilainen R, Heikinheimo M 2004 Transcription factors GATA-4 and GATA-6 in human adrenocortical tumors. Endocr Res 30:919–923
15. Dougherty SM, Mazhawidza W, Bohn AR, Robinson KA, Mattingly KA, Blankenship KA, Huff MO, McGregor WG, Klinge CM 2006 Gender difference in the activity but not expression of estrogen receptors α and β in human lung adenocarcinoma cells. Endocr Relat Cancer 13:113–134
16. Urahama N, Ito M, Sada A, Yakushijin K, Yamamoto K, Okamura A, Minagawa K, Hato A, Chihara K, Roeder RG, Matsui T 2005 The role of transcriptional coactivator TRAP220 in myelomonocytic differentiation. Genes Cells 10:1127–1137
17. Matsumoto K, Yu S, Jia Y, Ahmed MR, Viswakarma N, Sarkar J, Kashireddy PV, Rao MS, Karpus W, Gonzalez FJ, Reddy JK 2007 Critical role for transcription coactivator peroxisome proliferator-activated receptor (PPAR)-binding protein/TRAP220 in liver regeneration and PPARα ligand-induced liver tumor development. J Biol Chem 282:17053–17060
18. Guo D, Sarkar J, Ahmed MR, Viswakarma N, Jia Y, Yu S, Sambasiva Rao M, Reddy JK 2006 Peroxisome proliferator-activated receptor (PPAR)-binding protein (PBP) but not PPAR-interacting protein (PRIP) is required for nuclear translocation of constitutive androstane receptor in mouse liver. Biochem Biophys Res Commun 347: 485–495
19. Li JM, Wang XF, Xi ZQ, Gong Y, Liu FY, Sun JJ, Wu Y, Luan GM, Wang YP, Li YL, Zhang JG, Lu Y, Li HW 2006 Decreased expression of thyroid receptor-associated protein 220 in temporal lobe tissue of patients with refractory epilepsy. Biochem Biophys Res Commun 348:1389–1397
20. Rainey WE, Bird IM, Mason JI 1994 The NCI-H295 cell line: a pluripotent model for human adrenocortical studies. Mol Cell Endocrinol 100:45–50
21. Nakamura Y, Aoki S, Xing Y, Sasano H, Rainey WE 2007 Metastin stimulates aldosterone synthesis in human adrenal cells. Reprod Sci 14:836–845
22. Brewer A, Gove C, Davies A, McNulty C, Barrow D, Koutsourakis M, Farzaneh F, Pizzey J, Bomford A, Patient R 1999 The human and mouse GATA-6 genes utilize two promoters and two initiation codons. J Biol Chem 274:38004–38016
23. Nakamura Y, Gang HX, Suzuki T, Sasano H, Rainey WE 2009 Adrenal changes associated with adrenarche. Rev Endocr Metab Disord 10:19–26
24. Rainey WE, Viard I, Mason JI, Cochet C, Chambaz EM, Saez JM

1988 Effects of transforming growth factor β on ovine adrenocortical cells. Mol Cell Endocrinol 60:189–198
25. **Brewer A, Nemer G, Gove C, Rawlins F, Nemer M, Patient R, Pizzey J** 2002 Widespread expression of an extended peptide sequence of GATA-6 during murine embryogenesis and non-equivalence of RNA and protein expression domains. Mech Dev 119(Suppl 1): S121–S129
26. **Molkentin JD** 2000 The zinc finger-containing transcription factors GATA-4, -5, and -6. Ubiquitously expressed regulators of tissue-specific gene expression. J Biol Chem 275:38949–38952
27. **Wood JR, Nelson VL, Ho C, Jansen E, Wang CY, Urbanek M, McAllister JM, Mosselman S, Strauss 3rd JF** 2003 The molecular phenotype of polycystic ovary syndrome (PCOS) theca cells and new candidate PCOS genes defined by microarray analysis. J Biol Chem 278:26380–26390
28. **Qi C, Zhu Y, Reddy JK** 2000 Peroxisome proliferator-activated receptors, coactivators, and downstream targets. Cell Biochem Biophys 32:187–204
29. **Glass CK, Rosenfeld MG** 2000 The coregulator exchange in transcriptional functions of nuclear receptors. Genes Dev 14:121–141
30. **Rainey WE, Nakamura Y** 2008 Regulation of the adrenal androgen biosynthesis. J Steroid Biochem Mol Biol 108:281–286
31. **Shibata H, Ikeda Y, Mukai T, Morohashi K, Kurihara I, Ando T, Suzuki T, Kobayashi S, Murai M, Saito I, Saruta T** 2001 Expression profiles of COUP-TF, DAX-1, and SF-1 in the human adrenal gland and adrenocortical tumors: possible implications in steroidogenesis. Mol Genet Metab 74:206–216
32. **Hanley NA, Rainey WE, Wilson DI, Ball SG, Parker KL** 2001 Expression profiles of SF-1, DAX1, and CYP17 in the human fetal adrenal gland: potential interactions in gene regulation. Mol Endocrinol 15:57–68

The 14th International Thyroid Congress
September 11–16, 2010
Palais des Congrès, Paris, France

Website: http://www.itc2010.com

Contact information for Secretariat of Congress

ITC 2010-MCI Paris
24, rue Chauchat
75009 Paris
Tel : (01)1 53 85 82 80
Fax : (01)1 53 85 82 83
Email: ITC2010info@mci-group.com

Key dates:

- Second announcement & call for abstracts: November 2009
- Deadline for abstracts submission: 30 April 2010
- Deadline for early bird registration: 30 June 2010

Molecular and Cellular Endocrinology 307 (2009) 163–168

Contents lists available at ScienceDirect

Molecular and Cellular Endocrinology

journal homepage: www.elsevier.com/locate/mce

Transcriptional regulation of 17β-hydroxysteroid dehydrogenase type 12 by SREBP-1

Shuji Nagasaki[a,b], Yasuhiro Miki[a], Jun-ichi Akahira[a], Takashi Suzuki[a,c], Hironobu Sasano[a,*]

[a] Department of Pathology, Tohoku University Graduate School of Medicine, 2-1 Seiryo-machi, Aoba-ku, Sendai, Miyagi-ken, 980-8575, Japan
[b] Kawasaki Research Center, ASKA Pharmaceutical Co., Ltd., Kawasaki, Japan
[c] Department of Pathology and Histotechnology, Tohoku University Graduate School of Medicine, Sendai, Japan

ARTICLE INFO

Article history:
Received 18 December 2008
Received in revised form 2 March 2009
Accepted 4 April 2009

Keywords:
Fatty acid
SREBP-1
17β-Hydroxysteroid dehydrogenase type 12

ABSTRACT

17β-Hydroxysteroid dehydrogenase type 12 (17β-HSD12) has been demonstrated to be involved in enzymatic conversion of weak estrogen, estrone to more potent one, estradiol. However, this enzyme was also reported to be involved in an elongation of very long chain fatty acid (VLCFA). Many genes involved in lipid metabolism are regulated by the transcription factor termed sterol regulatory element-binding proteins (SREBPs). Results of our present study demonstrated that the existence of putative SRE sequence which is recognized as responsive element for SREBPs in 5′-flanking region of 17β-HSD12 gene. Results of luciferase assay demonstrated that the transcriptional activity of this SRE sequence depends on the activation of SREBP-1 in HepG2 (hepatocellular carcinoma cell line, human) and SK-BR-3 (breast carcinoma cell line, human). 17β-HSD12 expression was also induced in the HepG2 cells treated with the absence of sterols in which SREBPs were activated. All these results obtained in this study clearly indicate that SREBP-1 represents one of the transcriptional regulators of human 17β-HSD12.

1. Introduction

17β-Hydroxysteroid dehydrogenase type 12 (17β-HSD12) is one of the members of 17β-HSD family, which has been widely recognized to catalyze the reversible interconversions between biologically active and inactive sex steroid. Especially, 17β-HSD12 has been demonstrated to be involved in the conversion of weak estrogen, estrone (E1), to the more potent one, estradiol (E2) (Luu-The et al., 2006).

17β-HSD12 was also reported to be involved in very long chain fatty acid synthesis (C>18; VLCFA) (Moon and Horton, 2003). Sakurai et al. (2006) reported that 17β-HSD12 was abundantly expressed in organs involved in lipid metabolism such as liver, kidney, testis and placenta. In human breast carcinoma, which is considered one of estrogen dependent cancers, the level of 17β-HSD12 expression was relatively higher in carcinoma tissues than in non-malignant breast tissue (Song et al., 2006). The expression of this enzyme has been reported in human breast carcinoma, but 17β-HSD12 was in generally considered to be mainly involved in fatty acid synthesis rather than E2 synthesis (Day et al., 2008; Nagasaki et al., 2009). These data above all indicate that 17β-HSD12 is involved in fatty acid synthesis as well as in E2 synthesis.

Sterol regulatory element-binding proteins (SREBPs) belong to the members of the basic-helix–loop–helix-leucine zipper family of transcription factors which regulate biosynthesis of both cholesterol and fatty acids metabolism. The SREBP family members include SREBP-1a, SREBP-1c and SREBP-2 (Shimano, 2001). SREBP-1 isoforms preferentially activate the genes encoding fatty acid biosynthetic enzymes, whereas SREBP-2 tends to activate genes of cholesterol biosynthetic enzymes. SREBPs in general exist as inactive precursors bound to the endoplasmic reticulum (ER) membrane in the cells. These inactive precursors need to be proteolytically cleaved in Golgi apparatus, for an activation, to release the N-terminal active domain which sequentially enter into nucleus (designated nSREBPs), in which the activated forms bind to specific sterol response element (SRE) in the promoter region of the corresponding target genes. An activation of SREBPs is modulated by cellular sterol contents in order to maintain lipid homeostasis. Many genes involved in lipid metabolism, fatty acid and cholesterol biosynthesis have been reported to be under the regulation of SREBPs (Shimano, 2001).

All previously published studies indicated the possibility that the transcriptional regulation of 17β-HSD12 may also be regulated by SREBP-1. We therefore examined the mechanisms of transcriptional regulation of 17β-HSD12 in this study based on the hypothesis above. We first explore 5′-flanking region of the 17β-HSD12 gene for detecting SRE sequence in order to confirm whether this gene is also regulated by SREBPs. We detected the perfect consensus SRE sequence (Osborne et al., 1988), and its sequence

* Corresponding author. Tel.: +81 22 717 8050; fax: +81 22 717 8051.
E-mail address: hsasano@patholo2.med.tohoku.ac.jp (H. Sasano).

0303-7207/$ – see front matter © 2009 Elsevier Ireland Ltd. All rights reserved.
doi:10.1016/j.mce.2009.04.002

was identical to that of HMG-CoA synthase which is one of the well-known SREBP-regulated genes (Smith et al., 1988). We further evaluated whether the SRE sequence identified in 5′-flanking region of the 17β-HSD12 gene is responsible for the transcriptional regulation of this enzyme by SREBP-1 using luciferase reporter gene assay.

2. Materials and methods

2.1. Analysis of the 5′-flanking sequence

Potential binding site for SREBPs within the 1000 bp 5′-flanking region of 17β-HSD12 was predicted using TESS (http://www.cbil.upenn.edu/cgi-bin/tess/tess) in the combined strings and weight matrix search mode and TFSEARCH (http://www.cbrc.jp/research/db/TFSEARCHJ.html) with a default threshold setting 85.0 for the search.

2.2. Preparation of vector construct and site-directed mutagenesis

The 5′-flanking region of the 17β-HSD12 gene was amplified by PCR from HepG2 genomic DNA using a following primer with 5′-NheI and 3′-XhoI restriction site (underlined sequence): 5′-TT*GCTAGC*AGTCTCACTCCGTCGCTCAG-3′ (5′-primer), 5′-AG*CTCGAG*AGAGCGAGTGAATGAATCCAG-3′ (3′-primer). Genomic DNA was extracted using AquaPure Genomic DNA Isolation Kit (Bio-Rad Laboratories, Hercules, CA). The PCR product of 5′-flanking region (690 bp, −492 ~ +198) of the 17β-HSD12 gene was then cloned into the NheI and XhoI sites of pGL3 basic luciferase reporter vector (Promega, Madison, WI) and designated as pGL3/HSD17B12-492. The transcriptional active domain of SREBP-1a (aa 1-460) and SREBP-1c (aa 1-436) was amplified by PCR using the following primers with 5′-NheI and 3′-XhoI restriction site (underlined sequence): 5′-TT*GCTAGC*CATGGACGAGCCACCCTTC-3′ (5′-primer for SREBP-1a), 5′-AC*GCTAGC*CATGGATTGCACTTTCG-3′ (5′-primer for SREBP-1c) and 5′-AA*CTCGAG*TCAGTCAGGCTCCGAGTCACTGC-3′ (3′-primer for activation domain of SREBP-1a and SREBP-1c). The PCR product of the activation domain of SREBP-1a and 1c was subsequently cloned into the NheI and XhoI sites of pcDNA3.1 (−) (Invitrogen, Carlsbad, CA) and were designated as pcDNA3.1/nSREBP-1a and pcDNA3.1/nSREBP-1c respectively. The replacement mutation of SRE sequence of pGL3/HSD17B12-492 was created by site-directed mutagenesis using QuickChange Site-directed Mutagenesis Kit (Stratagene, La Jolla, CA) and designated as pGL3/HSD17B12-492 (m). The SRE sequence of pGL3/HSD17B12-492 5′-GTGGGGTGAGA-3′ was replaced by the sequence 5′-GTGAGATAAGA-3′. The sequences of the primers used to generate mutations are as follows (mutated bases are indicated in boldface): mSRE-5′, 5′-GGGGCGCCTCGGTG**AGATAA**GACAGGGCGCTCA-3′; m-SRE-3′, 5′-TGAGCGCCCTGTCT**TATCT**CACCGAGGCGCCCC-3′.

2.3. Cell culture

Human hepatoma cell line HepG2 and breast cancer cell line SK-BR-3 were cultured in RPMI-1640 supplemented with 10% fetal bovine serum at 37 °C under 5% CO_2 atmosphere. For inhibition of endogenous SREBP-1 activity, sterol (+) condition was established by an addition of 1 μg/mL 25-OH cholesterol and 10 μg/mL cholesterol to RPMI-1640 culture medium supplemented with lipid-depleted serum (Biowest, Miami, FL) according to the previous report (Shechter et al., 2003). For activation of SREBP-1, sterol (−) conditions was achieved by an addition of 5 μg/mL HMG-CoA reductase inhibitor, lovastatin, to remove cholesterol completely to RPMI-1640 culture medium supplemented with 10% lipid-depleted serum (Biowest) according to the previous report (Shechter et al., 2003).

2.4. RT-PCR analysis

HepG2 was seeded on 35 mm dish with RPMI-1640 supplemented with 10%FBS in 24 h before ±sterol treatment as described above. The culture media were changed to sterol (+) or sterol (−) medium as defined above at the time of treatment. The total RNA was extracted using TRIzol Reagent (Invitrogen) following the incubation for another 24 h, and cDNA was synthesized using QuantiTect reverse transcription kit (QIAGEN GmbH, Hilden, Germany). Real-time PCR was performed using the LightCycler System and FastStart DNA Master SYBR GreenI (Roche Diagnostics GmbH, Mannheim, Germany). The PCR primer sequence of 17β-HSD12, FASN, low-density lipoprotein receptor (LDLR), 3-hydroxy-3-methyl-glutaryl-CoA reductase (HMG-CoA reductase), and ribosomal protein L13A (RPL13A) used in this study was summarized as follows: 17β-HSD12 (NM_016142); forward 5′-GAGAGTGGGCAGTTGTCA-3′ and reverse 5′-CAGCAATGGTTCTTGTCTCC-3′, FASN (NM_004104); forward 5′-CATGGCAACGTGATGCTAC-3′ and reverse 5′-CGATGACGTGGACGGATACT-3′, LDLR (NM_000527); forward 5′-AGATGCGAAAGAAACCAG-3′ and reverse 5′-ATTTGCAGGTGACAGAGA- 3′, HMG-CoA reductase (NM_000859); forward 5′-GGCTCGAAACATCTGAAG-3′ and reverse 5′-CTGGACTGGAAACGGATA-3′, RPL13A (NM_ 012423); forward 5′-CCTGGAGGAGAAGAGGAAAGAGA-3′ and reverse 5′-TTGAGGACCTCTGTGTATTTGTCAA-3′. To determine the quantity of target cDNA transcript, cDNAs of known concentrations for target genes, and the housekeeping gene, RPL13A, were used to generate standard curves for real-time quantitative PCR. The mRNA level in each case was represented as a ratio of RLP13A and was evaluated as a ratio (%) compared with that of each control.

2.5. Immunoblot analysis

HepG2 cells were treated under ±sterol condition described above for 24 h in order to confirm SREBP-1 activation and 72 h for further confirmation of subsequent induction of 17β-HSD12 protein. Rabbit polyclonal antibody for 17β-HSD12 was raised against a peptide corresponding to the C-terminal residues of 17β-HSD12 (302-RAHYLKKTKKN-312). The characterization of the antibody employed in this study has been previously reported by using both immunoblotting and immunohistochemistry (Sakurai et al., 2006). Mouse monoclonal antibody for SREBP-1 (2A4) and β-actin (AC-15) were purchased from SantaCruz Biotechology (Santa Cruz, CA) and Sigma–Aldrich (St Louis, MO), respectively. Total protein of the cell was extracted using M-PER Mammalian Protein Extraction Reagent (Pierce Biotechnology, Rockford, IL) with Halt Protease Inhibitor Cocktail (Pierce Biotechnology). Both nuclear and cytoplasmic proteins were extracted using CelLytic NuCLEAR Extraction Kit (Sigma–Aldrich) according to instruction manual. The concentrations of the protein included in those lysate were measured using Protein Assay Kit Wako (Wako Pure Chemical Industries, Osaka, Japan). Nuclear (70 μg/lane), cytoplasmic (40 μg) and total protein (20 μg) were individually subjected to SDS–PAGE (10% acrylamide gel). Following SDS–PAGE, proteins were transferred onto Hybond P polyvinylidene difluoride membrane (GE Healthcare, Buckinghamshire, UK). The blots were then blocked in 5% non-fat dry skim milk for 1 h at room temperature, and were then incubated with a primary antibody for 17β-HSD12, SREBP-1 and β-actin for 24 h at 4 °C. Dilutions of primary antibodies used in this study were summarized as follows: 17β-HSD12; 1/1000, SREBP-1; 1/50 and β-actin; 1/1000. These antibody–protein complexes on the blots were detected using ECL-plus Western blotting detection reagents (GE Healthcare) following incubation with anti-mouse or anti-rabbit IgG horseradish peroxidase (GE Healthcare, Buckinghamshire, England) for 1 h at room temperature. The corresponding protein bands were subsequently visualized with LAS-1000 cooled CCD-camera chemiluminescent image analyzer (Fuji Photo Film Co., Tokyo, Japan).

2.6. Luciferase assay

HepG2 or SK-BR-3 cells were seeded in 5×10^4 or 1×10^5 cells/well in 24-well plate in RPMI-1640 medium supplemented with 10% FBS. After additional 24 h incubation, the cells were transfected with pSV-β-Galactosidase control vector (Promega), pGL3/HSD17B12-492 or pGL3/HSD17B12-492 (m) and pcDNA3.1/nSREBP-1a or pcDNA3.1/nSREBP-1c in several concentrations using *Trans*IT-LT1 Transfection Reagents (Mirus Bio Corporation) according to the manufacture's instruction. The whole cell lysate was prepared by PLB buffer (promega) after 24 h of transfection and activity of luciferase and β-galactosidase were subsequently measured using ONE-Glo Luciferase Assay System (Promega) and β-Galactosidase Enzyme Assay System (Promega) according to the manufacture's instruction. Relative luciferase activity is expressed as the ratio of luciferase activity to β-galactosidase activity. In the assay under ±sterol condition, cells were transfected with pGL3/HSD17B12-492 and pSV β-Galactosidase control vector (Promega), and then after 12 h of transfection, the culture medium were changed to sterol (+) or sterol (−) medium defined above to inhibit or activate SREBP-1. The whole cell lysate was prepared and applied to the measurements of luciferase and β-galactosidase activity as described above following further incubation for 24 h.

2.7. Chromatin immunoprecipitation (ChIP) assay

ChIP assay was performed using Chromatin Immunoprecipitation Assay Kit (Millipore, Billerica, MA). HepG2 cells were cultured with sterol (−) medium defined above for 24 h for activation of SREBP-1. Cells were cross-linked with 1% formaldehyde for 10 min at 37 °C. The cells were washed and scraped with cold PBS containing with Protease Inhibitor Cocktail (Pierce Biotechnology). Pellets were then dissolved with SDS buffer and sonicated to shear DNA. Protein–DNA complex was first pre-cleared for 1 h with Protein A Agarose/Salmon Sperm DNA. Supernatant was incubated with 3 μg of anti-SREBP-1 antibody (H160, Santa Cruz) or no antibody (mock condition) for 18 h at 4 °C with agitation. Antibody against SREBP-1 employed in this study (H160) was widely used in several previous studies for ChIP analysis of SREBP-1 (Dif et al., 2006; Gosmain et al., 2005). The immunoprecipitated complex obtained was bound to Protein A Agarose/Salmon Sperm DNA for 1 h at 4 °C and sufficiently washed with Wash buffers in order to reduce background signals. Protein–DNA complex was subsequently eluted from the immunoprecipitated complex by elution buffer (1% SDS, 0.1 M $NaHCO_3$, 10 mM DTT). 4 μL of 5 M NaCl was added to these elutes above (100 μL) and reverse protein–DNA crosslinks procedure was performed by heating at 65 °C for 6 h. 2 μL of 0.5 M EDTA, 4 μL of 1 M Tris–HCl, pH 6.5 and 0.6 μL of 6 mg/mL Proteinase K were subsequently added to these elutes and were further incubate for 1 h at 45 °C. DNA was purified using PCR purification kit (Qiagen) and was eluted in 50 μL water. The set of PCR primers used in this study of the human 17β-HSD12 proximal promoter were summarized as follows: 5′-primer, 5′-AATCCGAGCGCAGTCTTCC-3′; 3′-primer, 5′-GCCATTAGCTGACTCCAGTTCC-3′. PCR amplification products were analyzed on ethidium bromide-stained 2%-agarose gels.

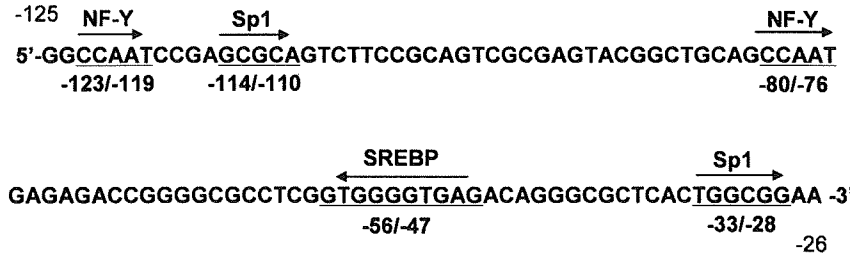

Fig. 1. 5'-Flanking sequence of human 17β-HSD12 gene. Results of database analysis indicated that the existence of putative SRE (−56/−47) sequence and binding site of NF-Y (−123/−119, −80/−76)) and Sp1 (−114/−110, −33/−28).

2.8. Statistical analysis

Statistical differences were examined using the StatView 5.0J software (SAS Institute, Cary, NC). Results were expressed as mean ± SD, and analyzed by Student's *t*-test. A *p*-value <0.05 was considered statistical significance in all these analyses above.

3. Results

3.1. Predicted binding sites of SREBPs

We identified a putative SRE sequence at nucleotide position −56/−47 in a reverse orientation (5'-GTGGGGTGAG-3') (Fig. 1) as a result of prediction of potential binding site for SREBPs using TESS and TFSERACH. In addition, we also identified the estimated binding sites of NF-Y and Sp1 in the vicinity of SRE sequence at nucleotide position −80/−76 and −33/−28 respectively (Fig. 1).

3.2. Increased expression of 17β-HSD12 by activation of SREBPs

Results of immunoblot analysis demonstrated that the SREBP-1 protein was detected in cytoplasmic fraction containing ER in +sterol condition, and also detected in a nucleus in −sterol condition (Fig. 2B). Results of RT-PCR analysis revealed that the mRNA expression of HMG-CoA reductase, LDLR and FASN, all of which are well-known representative genes regulated by SREBPs was induced under the −sterol condition in which SREBP-1 was activated (Fig. 2A). The expression of 17β-HDS12 was also significantly induced with approximately 3-fold in −sterol condition compared to +sterol (Fig. 2A). Results of immunoblot analysis also demonstrated that 17β-HSD12 protein is induced in −sterol condition cultured for 72 h (Fig. 2C).

3.3. SRE sequence dependent transcriptional regulation by SREBP-1

Results of the luciferase assay using HepG2 and SK-BR-3 cells co-transfected with pGL3/HSD17B12-492 and pcDNA3.1/nSREBP-1c were summarized in Fig. 3. The expression of nSREBP-1c resulted in intense increment of the luciferase activity of the lysate, and its activity was decreased according to reduced amounts of nSREBP-1c transfection (Fig. 3B and C) in both cell line. Results of the assay using nSREBP-1a demonstrated similar results (data not shown). The results of the assay using HepG2 cells transfected with pGL3/HSD17B12-492 but without nSREBP-1 demonstrated relatively high luciferase activity compared to that transfected with pGL3 basic vector (promoter region is not introduced). This relatively high promoter activity was not detected in the assay using SK-BR-3 cell.

We subsequently examined whether this luciferase activity induced by SREBP-1 expression depends on SRE sequence or not using site-directed mutagenesis method. In this particular examination, we used only SREBP-1a expression vector because the

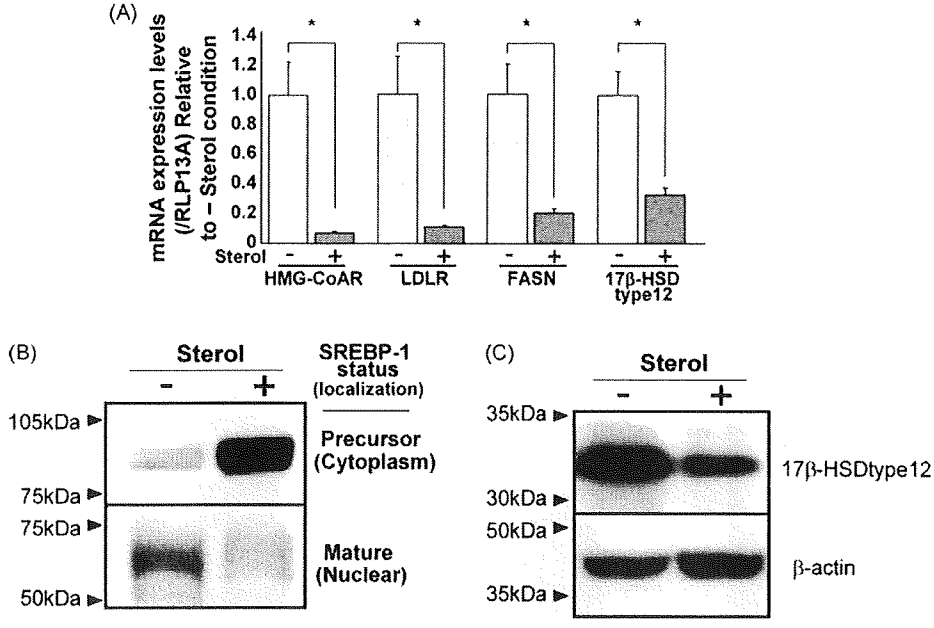

Fig. 2. SREBP-regulated genes expression in response to sterol conditions of the medium. In RT-PCR analysis, HepG2 cells were treated with ±sterol condition for 24 h and applied to the assay (A). Data are shown as mean ± S.D. ($n = 3$). *$p < 0.05$. HepG2 cells were treated with ±sterol condition for 24 h and cytoplasmic and nuclear protein were applied to the assay (B) in immunoblot analysis for SREBP-1. HepG2 cells were treated with ±sterol condition for 72 h (C) in order to detect an alteration in 17β-HSD12 protein.

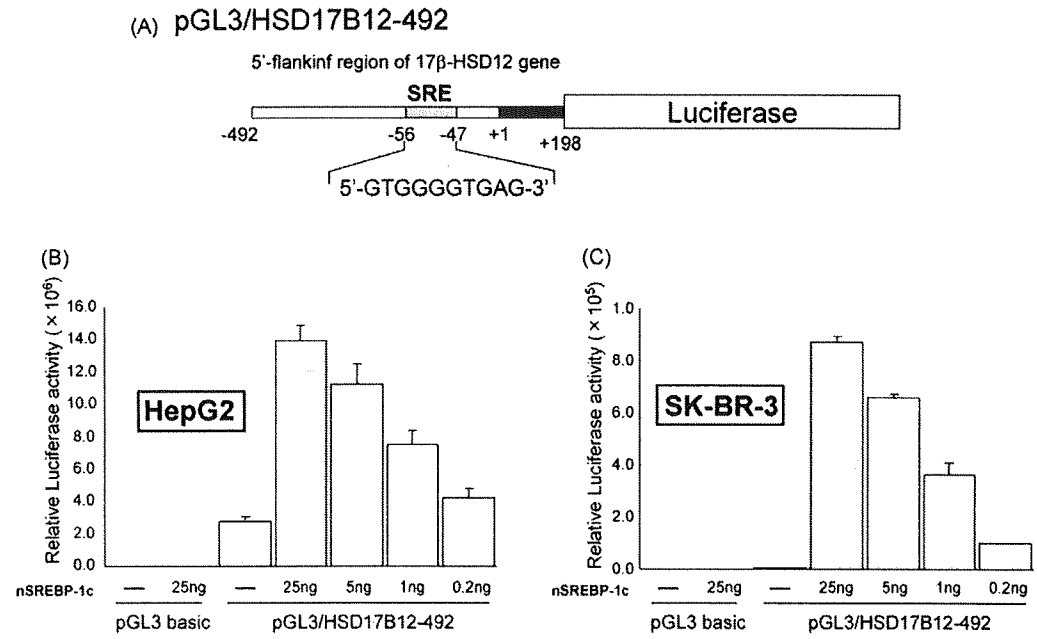

Fig. 3. nSREBP-1 dependent regulation of 5′-flanking region of 17β-HSD12 gene. Construction of reporter vector designated as pGL3/HSD17B12 was shown in (A). The luciferase activity of HepG2 (B) and SK-BR-3 (C) transfected with pGL3/HSD17B12-492 and pcDNA3.1/nSREBP-1c was determined in 24 h after transfection. Data are shown as mean ± S.D. ($n = 3$).

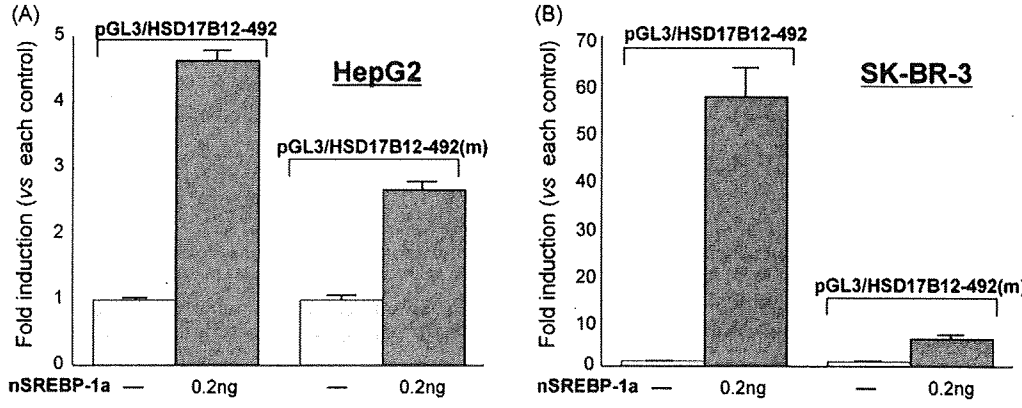

Fig. 4. Mutational analysis of the sequence dependent SRE activity. HepG2 (A) and SK-BR-3 (B) were transfected with pGL3/HSD17B12-492 or pGL3/HSD17B12 (m) and pcDNA3.1/nSREBP-1a. Luciferase activity was then measured in 24 h after transfection. Data are shown as mean ± S.D. ($n = 3$).

structural difference between SREBP-1a and -1c is just only on transcriptional activation region located in N-terminal but not on DNA binding domain located in C-terminal. The luciferase activity of the lysate of the cells transfected with pGL3/HSD17B12-492 was intensively increased by the expression of nSREBP-1a but that of the cells transfected with pGL3/HSD17B12-492 (m) was marginally induced in both cell lines (Fig. 4A and B). In addition, the luciferase activity in the cells transfected with pGL3/HSD17B12-492 was also induced

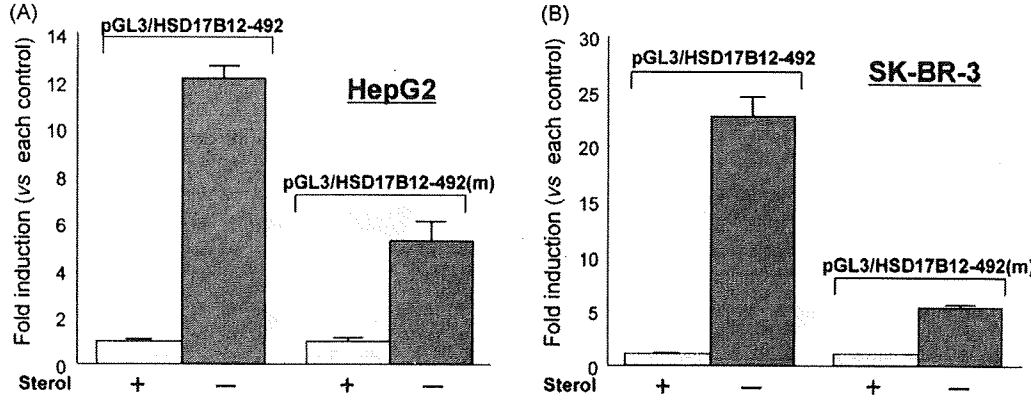

Fig. 5. Sterol responsive regulation of 5′-flanking region of 17β-HSD12 gene. HepG2 (A) and SK-BR-3 (B) were transfected with pGL3/HSD12-492 or pGL3/HSD17B12 (m), and were treated with ±sterol condition for 24 h. Luciferae activity was determined and data are shown as mean ± S.D. ($n = 3$).

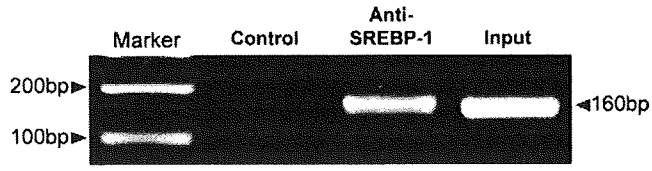

Fig. 6. Binding of SREBP-1 on the sequence containing SRE. HepG2 cells were treated with −sterol condition of the medium for 24 h and were further applied to ChIP analysis. Samples, no antibody control (Control), immunoprecipitated with SREBP-1 specific antibody (anti-SREBP-1) and not treated with immunoprecipitation (Input) were applied in PCR and electrophoresis was performed with 2.0% agarose gel.

under −sterol condition compared to +sterol condition, however, that of the cells transfected with pGL3/HSD17B12-492 (m) was marginally induced in both cell lines (Fig. 5A and B).

3.4. Binding of SREBP-1 to SRE

Results of ChIP assay were summarized in Fig. 6. The HepG2 cells were treated under −sterol condition for 24 h and applied to the ChIP assay. Results of the PCR following immunoprecipitation by anti-SREBP-1 antibody and those of the sample before immunoprecipitation (input) revealed the single distinct band at the estimated size in electrophoresis and no bands at an unexpected size were observed. PCR product was purified and verified by sequencing analysis. There were, however, no discernible bands in the PCR study using negative control sample which is treated without antibody.

4. Discussion

Results of database analysis of 5′-flanking region of 17β-HSD12 gene in our present study revealed the existence of putative SRE sequence at the position −56/−47 (Fig. 1). In addition, this sequence was identical to the consensus SRE sequence (Osborne et al., 1988) and to that of HMG-CoA synthetase which is one of the most characterized SREBP-regulated genes (Smith et al., 1988). We also identified deduced binding sequence of NF-Y (−80/−76) and Sp1 (−33/−28) in the vicinity of SRE, both of which are known as one of the ubiquitously expressed transcription factors and generally considered to be required for recruitment and stabilization of the SREBPs interaction and to activate the promoter (Edwards and Ericsson, 1999; Xiong et al., 2000). Therefore, these structural features of the 5′-flanking region of 17β-HSD12 gene clearly demonstrated that 17β-HSD12 is regulated by SREBP. Results of immunoblot analysis demonstrated that SREBP-1 was cleaved and activated in the HepG2 cells treated with −sterol condition (Fig. 2B). In this condition, 17β-HSD12 mRNA expression was also significantly increased, as well as other SREBP-regulated genes such as LDLR (Sudhof et al., 1987), HMG-CoA reductase (Osborne et al., 1985) and FASN (Bennett et al., 1995) (Fig. 2A). These data above all suggested that the expression of 17β-HSD12 is actually regulated by SREBPs, in the same fashion as in the cases of other SREBP-regulated genes.

We then performed luciferase assay in order to clarify whether the SRE sequence identified in 5′-flanking region of 17β-HSD12 gene may be regulated by SREBP-1 or not. Results of several studies demonstrated that the almost all SRE identified in the promoter regions of SREBP-regulated genes is located between within −400 to +1 region, and enough to regulate the expression of these genes in response to changes in lipid condition (Bennett et al., 1995; Smith et al., 1988; Shechter et al., 2003; Kumadaki et al., 2008; Osborne et al., 1988). Therefore, in this study, we first constructed the reporter vector which contain 5′-flanking region of 17β-HSD12 position at −492/+198 containing putative SRE sequence identified in database analysis (Fig. 3A). In the assay using the co-transfection with pGL3/HSD17B12-492 and pcDNA3.1/nSREBP-1c to HepG2 and SK-BR-3 cells, the luciferase activity was clearly induced by nSREBP-1c expression (Fig. 3B and C). This increased luciferase activity was also detected by activation of endogenous SREBPs (Fig. 5). In addition, this activation was clearly dependent on SRE sequence demonstrated by mutation analysis (Figs. 4 and 5). In ChIP analysis, we could demonstrate that endogenous nSREBP-1 bind to genomic DNA fragment containing SRE sequence identified in 17β-HSD12 promoter region. These results above all clearly indicated that the expression of 17β-HSD12 is directly regulated by SREBP-1 via the binding of nSREBP-1 on SRE sequence at the position −56/−47 of 5′-flanking region of 17β-HSD12 gene.

Moon and Horton (2003) reported that the expression of 17β-HSD12 mRNA was not increased in the liver of transgenic mouse in which nSREBP-1a or -1c was expressed. The discrepancy of the results between the study of transgenic mouse above and our present study may be due to the difference of species between rodents and primates but it requires further investigations for clarification.

Relatively intense increment of luciferase activity in HepG2 cells transfected with only pGL3/HSD17B12-492 was observed even though nSREBP-1 expression vector was not expressed (Fig. 3B). Results of this assay also suggest that, at least in liver, the transcriptional regulation of 17β-HSD12 by SREBP-1 may minor mechanism and the liver specific factor constitutively activate this promoter via a sequence other than SRE. Indeed, under ±sterol condition, the changes of 17β-HSD12 mRNA were modest compared to other SREBP regulated genes in HepG2 cells (Fig. 2A). Meanwhile, the regulation of 17β-HSD12 expression might be critical mechanism in breast cancer cell line such as SK-BR-3 in which promoter activity of 5′-flanking region of 17β-HSD12 was highly dependent on the expression of nSREBP-1 (Fig. 3A).

Results of our previous studies demonstrated that the increased 17β-HSD12 expression in breast cancer cells contributes to cancer cell progression via fatty acid synthesis and its expression was correlated with the survival of the patients (Nagasaki et al., 2009). Therefore, results of our present study could provide potentially important information as to further understanding of the regulation and role of 17β-HSD12 in human breast carcinoma.

In summary, results of our present study indicated that the expression of the 17β-HSD12 is directly regulated by SREBP-1.

Acknowledgements

This work was partly supported by the grants from the Japanese Ministry of Health, Labour and Welfare for Researches on Intractable Diseases, Risk Analysis Research on Food and Pharmaceuticals, and Development of Multidisciplinary Treatment Algorithm with Biomarkers and Modeling of the Decision-making Process with Artificial Intelligence for Primary Breast Cancer. This work was also partly supported by Grant-in-Aid for Scientific Research (18390109) from the Japanese Ministry of Education, Culture, Sports, Science and Technology, and the Yasuda Medical Foundation.

References

Bennett, M.K., Lopez, J.M., Sanchez, H.B., Osborne, T.F., 1995. Sterol regulation of fatty acid synthase promoter. Coordinate feedback regulation of two major lipid pathways. J. Biol. Chem. 270, 25578–25583.

Day, J.M., Foster, P.A., Tutill, H.J., Parsons, M.F., Newman, S.P., Chander, S.K., Allan, G.M., Lawrence, H.R., Vicker, N., Potter, B.V., Reed, M.J., Purohit, A., 2008. 17beta-hydroxysteroid dehydrogenase type 1, and not type 12, is a target for endocrine therapy of hormone-dependent breast cancer. Int. J. Cancer 122, 1931–1940.

Dif, N., Euthine, V., Gonnet, E., Laville, M., Vidal, H., Lefai, E., 2006. Insulin activates human sterol-regulatory-element-binding protein-1c (SREBP-1c) promoter through SRE motifs. Biochem. J. 400, 179–188.

Edwards, P.A., Ericsson, J., 1999. Sterols and isoprenoids: signaling molecules derived from the cholesterol biosynthetic pathway. Annu. Rev. Biochem. 68, 157–185.
Gosmain, Y., Dif, N., Berbe, V., Loizon, E., Rieusset, J., Vidal, H., Lefai, E., 2005. Regulation of SREBP-1 expression and transcriptional action on HKII and FAS genes during fasting and refeeding in rat tissues. J. Lipid Res. 46, 697–705.
Kumadaki, S., Matsuzaka, T., Kato, T., Yahagi, N., Yamamoto, T., Okada, S., Kobayashi, K., Takahashi, A., Yatoh, S., Suzuki, H., Yamada, N., Shimano, H., 2008. Mouse Elovl-6 promoter is an SREBP target. Biochem. Biophys. Res. Commun. 368, 261–266.
Luu-The, V., Tremblay, P., Labrie, F., 2006. Characterization of type 12 17beta-hydroxysteroid dehydrogenase, an isoform of type 3 17beta-hydroxysteroid dehydrogenase responsible for estradiol formation in women. Mol. Endocrinol. 20, 437–443.
Moon, Y.A., Horton, J.D., 2003. Identification of two mammalian reductases involved in the two-carbon fatty acyl elongation cascade. J. Biol. Chem. 278, 7335–7343.
Nagasaki, S., Suzuki, T., Miki, Y., Akahira, J., Kitada, K., Ishida, T., Handa, H., Ohuchi, N., Sasano, H., 2009. 17Beta-hydroxysteroid dehydrogenase type 12 in human breast carcinoma: a prognostic factor via potential regulation of fatty acid synthesis. Cancer Res. 69, 1392–1399.
Osborne, T.F., Goldstein, J.L., Brown, M.S., 1985. 5′ end of HMG CoA reductase gene contains sequences responsible for cholesterol-mediated inhibition of transcription. Cell 42, 203–212.
Osborne, T.F., Gil, G., Goldstein, J.L., Brown, M.S., 1988. Operator constitutive mutation of 3-hydroxy-3-methylglutaryl coenzyme A reductase promoter abolishes protein binding to sterol regulatory element. J. Biol. Chem. 263, 3380–3387.
Sakurai, N., Miki, Y., Suzuki, T., Watanabe, K., Narita, T., Ando, K., Yung, T.M., Aoki, D., Sasano, H., Handa, H., 2006. Systemic distribution and tissue localizations of human 17beta-hydroxysteroid dehydrogenase type 12. J. Steroid Biochem. Mol. Biol. 99, 174–181.
Shechter, I., Dai, P., Huo, L., Guan, G., 2003. IDH1 gene transcription is sterol regulated and activated by SREBP-1a and SREBP-2 in human hepatoma HepG2 cells: evidence that IDH1 may regulate lipogenesis in hepatic cells. J. Lipid Res. 44, 2169–2180.
Shimano, H., 2001. Sterol regulatory element-binding proteins (SREBPs): transcriptional regulators of lipid synthetic genes. Prog. Lipid Res. 40, 439–452.
Smith, J.R., Osborne, T.F., Brown, M.S., Goldstein, J.L., Gil, G., 1988. Multiple sterol regulatory elements in promoter for hamster 3-hydroxy-3-methylglutaryl-coenzyme A synthase. J. Biol. Chem. 263, 18480–18487.
Song, D., Liu, G., Luu-The, V., Zhao, D., Wang, L., Zhang, H., Xueling, G., Li, S., Desy, L., Labrie, F., Pelletier, G., 2006. Expression of aromatase and 17beta-hydroxysteroid dehydrogenase types 1, 7 and 12 in breast cancer. An immunocytochemical study. J. Steroid Biochem. Mol. Biol. 101, 136–144.
Sudhof, T.C., Van der Westhuyzen, D.R., Goldstein, J.L., Brown, M.S., Russell, D.W., 1987. Three direct repeats and a TATA-like sequence are required for regulated expression of the human low density lipoprotein receptor gene. J. Biol. Chem. 262, 10773–10779.
Xiong, S., Chirala, S.S., Wakil, S.J., 2000. Sterol regulation of human fatty acid synthase promoter I requires nuclear factor-Y- and Sp-1-binding sites. Proc. Natl. Acad. Sci. U.S.A. 97, 3948–3953.

ANTICANCER RESEARCH 29: 2525-2530 (2009)

Expression of Thymidine Phosphorylase and Dihydropyrimidine Dehydrogenase in Human Breast Carcinoma Cells and Tissues

WINGS T.Y. LOO[1,2], LOUIS W.C. CHOW[2], TAKASHI SUZUKI[1], KATSUHIKO ONO[1], TAKANORI ISHIDA[3], HISASHI HIRAKAWA[4], NORIAKI OHUCHI[3] and HIRONOBU SASANO[1]

[1]*Department of Pathology, Tohoku University Graduate School of Medicine, Sendai, Japan;*
[2]*UNIMED Medical Institute, Hong Kong, PRC;*
Departments of Surgery, [3]*Tohoku University School of Medicine, and* [4]*Tohoku Kosai Hospital, Sendai, Japan*

Abstract. *Background: The therapeutic effects of oral capecitabine are proposed to be determined by the equilibrium of two intratumoral metabolizing enzymes, namely thymidine phosphorylase (TP) and dihydropyrimidine dehydrogenase (DPD). The present study aims to evaluate this hypothesis by in vivo experiments and immunohistochemical analysis in 31 cases of human breast carcinoma. Materials and Methods: The effects of capecitabine on two breast carcinoma cell lines were evaluated by the status of both cell proliferation and apoptosis and mRNA levels of TP and DPD were also determined. TP and DPD status was determined by immunohistochemistry in 31 cases of breast carcinoma tissues and the results were compared with their clinicopathological parameters. Results: The therapeutic efficacy of capecitabine in two cell lines was not related to the levels of TP and DPD mRNA expression. No statistically significant association was detected between the status of these enzymes and the clinicopathological factors. Conclusion: In vitro study demonstrated that capecitabine was effective against the BT-483 and MB-MDA-231 breast carcinoma cell lines used but the significance of the status of intratumoral TP and DPD in determining its therapeutic efficacy needs further studies.*

Breast carcinoma is the most common malignancy of women in the great majority of developed countries and is also a leading cause of female mortality, with over 300,000 deaths annually (1). capecitabine is a relatively novel orally administered fluoropyrimidine carbonate primarily designed for the treatment of breast and colorectal carcinomas. In contrast to parenterally administered 5-fluorouracil (5-FU), oral capecitabine concentrates predominantly in tumor tissue compared to adjacent non-neoplastic tissues and plasma (2). Therefore, orally administered capecitabine enables physicians treating breast carcinoma to mimic the effects of continuous infusion 5-FU but in a convenient outpatient setting (3). Capecitabine has been recently proposed as a potential alternative for 5-FU therapy (4) because of reduced toxicity and ease of administration (5). The monotherapy regimen of capecitabine also demonstrated a favorable tolerability profile, with a notably lower incidence of myelosuppression in the patients treated with this agent as a monotherapy compared to the single use of other chemotherapeutic agents (6). Capecitabine, a TP-activated fluoropyrimidine, was rationally designed to generate 5-FU preferentially *in situ* or at the tumor site as a prodrug (7). 5-FU is well-known to be either catabolized by DPD or anabolized by TP (8). The former enzyme is responsible for detoxification and subsequent elimination of the agent, while the anabolic pathway forms the compounds responsible for cytotoxic activity toward carcinoma cells (8). TP has been demonstrated to be overexpressed in various human tumors and also to play an important role in angiogenesis, tumor growth, invasion and metastasis (9, 10). DPD is the initial and rate-limiting enzyme in the (fluoro) pyrimidine catabolic pathway. Tumor DPD levels were postulated to predict the clinical response to 5-FU-based therapy (11). Therefore, the purpose of our present study investigates the possible correlation between the levels of TP/DPD and therapeutic efficacy of capecitabine as a single agent in human breast carcinoma cell lines. In addition, the significance of TP/DPD status in human breast carcinoma was also evaluated by studying their correlation with clinicopathological parameters of the patients with invasive ductal carcinoma of the breast.

Correspondence to: Wings T.Y. Loo, UNIMED Medical Institute, 10/F, 72 Gloucester Road, Wanchai, Hong Kong, PRC. Tel: +852 28610286, Fax: +852 28611386, e-mail: tyloo@hku.hk

Key Words: Capecitabine, thymidine phosphorylase, dihydropyrimidine dehydrogenase, cell proliferation, apoptosis.

Materials and Methods

Preparation of chemotherapeutic drugs. The powder form of active capecitabine was kindly donated by Roche Company (Basel, Switzerland). It was dissolved in methanol and diluted with Hank's balanced salt solution (HBSS; Invitrogen, USA) prior to use.

Cell proliferation rate measured by WST-1 for capecitabine in breast carcinoma cells. Two breast cancer cell lines BT-483 and MB-MDA-231 (American Type Culture Collection (ATCC), Manassas, USA) were cultured. BT-483 is an estrogen-responsive cell line, whereas MB-MDA-231 is non-estrogen responsive. The culture medium and conditions were based on the ATCC instructions. The concentration for capecitabine was determined on the basis of the preliminary or pilot studies in order to determine the optimal and minimal inhibitory concentrations (data not presented). Hence, the optimal concentration of pre-activated capecitabine was 1 μg/ml (14). The cells were cultured in a 4-well slide in different groups. Cytotoxicity of capecitabine was assessed using cell proliferation reagent WST-1 (Roche Diagnostics, Mannheim, Germany). Cells were cultured at a density of 4,000 cells per well in 96-well microtitre plates. After the treatment with 1 μg/ml pre-activated capecitabine for 24 hours, WST-1 was applied and cells were incubated according to the instructions of the manufacturer. The optical density (OD) was read at 450 nm by a microplate reader (Sunrise, TECAN, Austria).

In situ TUNEL assay. After treatment with 1 μg/ml pre-activated capecitabine for 24 hours, a designated harvest time-points, cells were then fixed with 4% paraformaldehyde overnight at 4˚C prior to the application of Apoptag Peroxidase *In Situ* Apoptosis Detection Kit (Intergen, NY, USA). The assay was performed according to the manufacturer's instructions. The slides were finally counterstained with hematoxylin. The positive control slides included in the kit were stained as described. Negative controls were evaluated by substituting TdT with PBS in the process of staining. The evaluation of TUNEL assay was performed by counting numbers of positively stained cells from 200 cells in each of 10 different fields. Results were subsequently analyzed by Coolsnap Capture system (Roper Scientific Inc., USA), and Image analyzer (Metamorph-Winshell, Universal Imaging Corporation, USA).

Patient selection and tissue collection for TP and DPD analysis. From 2001 to 2004, a total of 31 surgical pathology specimens of the breast invasive ductal carcinoma were retrieved from surgical pathology or archival files of Tohoku University Hospital and Tohoku Kosai Hospital (Sendai, Japan) (Tables I and II). The Ethics Committees at Tohoku University School of Medicine and Tohoku Kosai Hospital approved the research protocols (#2005-68), with informed consent being obtained from these patients before surgery.

Immunohistochemistry. Mouse anti-human TP monoclonal antibody (1C6-203) and rat anti-human DPD monoclonal antibody (2H9-1b) were selected (Chugai Pharmaceutical Co., Tokyo, Japan). A Histofine Kit (Nichirei, Tokyo, Japan), which employs the streptavidin-biotin amplification method (12), was used for the identification of TP, ER, PR, Ki-67, and HER-2/neu immunoreactive staining (12), whereas DAKO CSA System (DAKO) was used for DPD immunohistochemical analysis (13). Antigen retrieval was performed according to the manufacturers' instructions. The dilutions of the primary antibodies were as follows: 1/1,000 TP; 1/50 ER; 1/30 PR; 1/50 Ki-67 and 1/200 HER-2/neu. Staining was completed by a 5-minute incubation with diaminobenzidine tetrahydrochloride. Finally, slides were counterstained with hematoxylin, and mounted with coverlips.

Scoring of immunoreactivity in TP and DPD analysis. TP and DPD immunoreactivity was detected in the cytoplasm of carcinoma cells. ER, PR, Ki-67 and HER-2/neu immunoreactivity was detected in the nuclei of carcinoma cells. The immunoreactivity was evaluated in more than 1,000 carcinoma cells for each case. Cases associated with a labeling index of less than 10% were tentatively designated negative.

Total RNA extraction and qRT-PCR for evaluation of TP and DPD mRNA expression. BT-483 and MB-MDA-231 cells were used as described in addition to the cases examined for immunohistochemistry. Breast carcinoma specimens had been immediately frozen in liquid nitrogen in the operating theatre and stored at –80˚C until RNA isolation. RNA was extracted from 31 cases in which immunohistochemistry of TP and DPD was performed, as well as from the two breast carcinoma cell lines. Total RNA was extracted by homogenizing frozen tissue samples or breast carcinoma cell lines in 1 ml TRIzol reagent (Life Technologies, Inc., USA) followed by a phenol-chloroform phase extraction and isopropanol precipitation. All RNA specimens were quantified by spectrophotometry and processed for reverse-transcription (RT). All the specimens were tested by one-step TP and DPD PCR assays using LightCycler TP mRNA Quantification Kit^{PLUS} and LightCycler DPD mRNA Quantification Kit^{PLUS} with LightCycler system (Roche Diagnostics). The reference gene used was Ribosomal protein L13a (*RPL13A*), for the correct normalization of gene expression analysis (15). The amplicon sizes were: TP=108 bp, DPD=148 bp and RPL13A=125 bp according to the manufacturer's instructions. A positive control RNA (calibrator, from the LC-mRNA quantification kits for TP and DPD) was also employed in the assay. The mRNA levels of *TP* and *DPD* in each case are normalized as a ratio of calibrator (arbitrary units).

Statistical analysis. Statistical significance of data obtained were analyzed by SPSS 15.0 (Chicago, Illinois, USA).

Results

Cell proliferation rate measured by WST-1 in breast carcinoma cells treated with capecitabine. Results obtained were essentially the same in the two cell lines. The proliferation rates for the capecitabine-treated groups examined were less than those of the controls, and were statistically significantly different (Table III).

In situ TUNEL assay. Under light microscopic evaluation, apoptosis-related morphological changes including cell shrinkage and condensation of cytoplasm and chromatin were detected. Apoptotic bodies, *i.e.* small cell fragments containing fragmented nuclei, were also detected. The mean percentage of apoptotic cells determined by TUNEL assay in the capecitabine-treated group was 11.18% in MB-MDA-231 cells and 8.46±0.34% in BT-483 cells.

Immunohistochemistry of TP and DPD in human breast carcinoma specimens. TP immunoreactivity was detected in the cytoplasm of carcinoma cells and was detected in 13 out of 31 breast carcinomas examined in this study (Figure 1). TP immunoreactivity was also partially detected in morphologically non-neoplastic ductal epithelial cells (Figure 1). TP

Table I. *Association between TP immunoreactivity and clinicopathological parameters in 31 breast carcinoma cases.*

	TP immunoreactivity		*P*-value
	+ (n=13)	– (n=18)	
Age (years)*	59.83	53.8±3.0	0.2275
Menopausal status			
Premenopausal	3	7	
Postmenopausal	10	11	0.5806
Tumor size (mm)*	31.5±4	30.1±4.6	0.8345
Lymph node status			
Positive	10	10	
Negative	3	8	0.3904
Histological grade			
1	3	0	
2	7	11	
3	3	7	0.0904
ERa status			
Positive	9	13	
Negative	4	5	0.9999
ERa LI*	47.2±11.4	44.8±8.7	0.8717
PR LI*	37.8±10.4	38.8±7.9	0.9394
HER2			
Positive	3	6	
Negative	10	12	0.8159
Ki-67 LI*	16.2±3.4	25.4±3.0	0.0523
TP mRNA*	13.6±2.2	8.0±1.0	0.0178
DPD			
Positive	9	6	
Negative	4	12	0.1050

*Data are presented as mean±95% confidence interval (95% CI). LI, labeling index. All other values represent the number of cases.

Table II. *Association between DPD immunoreactivity and clinicopathological parameters in 31 breast carcinomas.*

	DPD immunoreactivity		*P*-value
	+ (n=15)	– (n=16)	
Age (years)*	52.8±3.2	59.6±3.4	0.1580
Menopausal status			
Premenopausal	7	3	
Postmenopausal	8	13	0.1972
Tumor size (mm)*	32.8±4.3	28.4±4.9	0.5091
Lymph node status			
Positive	10	10	
Negative	5	6	0.9999
Histological grade			
1	2	1	
2	10	8	
3	3	7	0.3369
ERa status			
Positive	12	10	
Negative	3	6	0.4904
ERa LI*	55.5±9.9	36.8±9.4	0.1805
PR LI*	41.5±10.03	35.6±7.5	0.6444
HER2			
Positive	3	6	
Negative	12	10	0.4904
Ki-67 LI*	20.4±2.9	22.6±3.7	0.6434
DPD mRNA*	34.9±4.7	27.1±6.2	0.3328

*Data are presented as mean±95% confidence interval (95% CI). All other values represent the number of cases.

immunoreactivity was not detected in other components of the tissue such as intratumoral stromal cells and adipocytes of the specimens (Figure 1). No statistically significant association was detected between the status of TP immunoreactivity and clinicopathological factors examined (Table I).

DPD immunoreactivity was detected in the cytoplasm of both carcinoma and intratumoral stromal cells (Figure 1). DPD immunoreactivity was detected in 15 out of 31 breast carcinoma cases examined. DPD immunoreactivity was absent from adipocytes and non-neoplastic ductal epithelial cells (Figure 1). No statistically significant association was detected between the status of DPD immunoreactivity in both carcinoma cells and intratumoral stromal cells, and any of the clinicopathological factors examined (Table II). There were no correlations between the status of TP and DPD immunoreactivity in the 31 breast carcinoma specimens examined (Table I).

mRNA expression of TP and DPD in breast carcinoma cell lines. mRNA expression of *TP* and *DPD* in BT-483 and MB-MDA-231 was determined by quantitative RT-PCR analysis.

Table III. *The proliferation of MB-MDA-231 and BT-483 cell lines treated with capecitabine evaluated by WST-1 assay with comparison to control group.*

Cell lines	Group	Mean optical density	Std. deviation	*P*-value
MB-MDA-231	Control	0.287375	0.0326	
	Capecitabine	0.260812	0.0167	0.00012
BT-483	Control	0.477187	0.1022	
	Capecitabine	0.345031	0.0338	0.0000000026

The relative level of *TP* mRNA expression (arbitrary unit, AU) in BT-483 cells (0.405AU) was higher than that in MDA-MB-231 cells (0.0606 AU). The relative level of *DPD* mRNA in MDA-MB-231 cells (0.158 AU) was higher than that in BT-483 cells (0.0152 AU).

Discussion

Capecitabine is a useful antitumor agent against breast carcinoma cells and human fresh tissues on their inhibition of cell proliferation and metabolic rate, respectively (14, 16). Capecitabine effectively inhibited the cell proliferation of

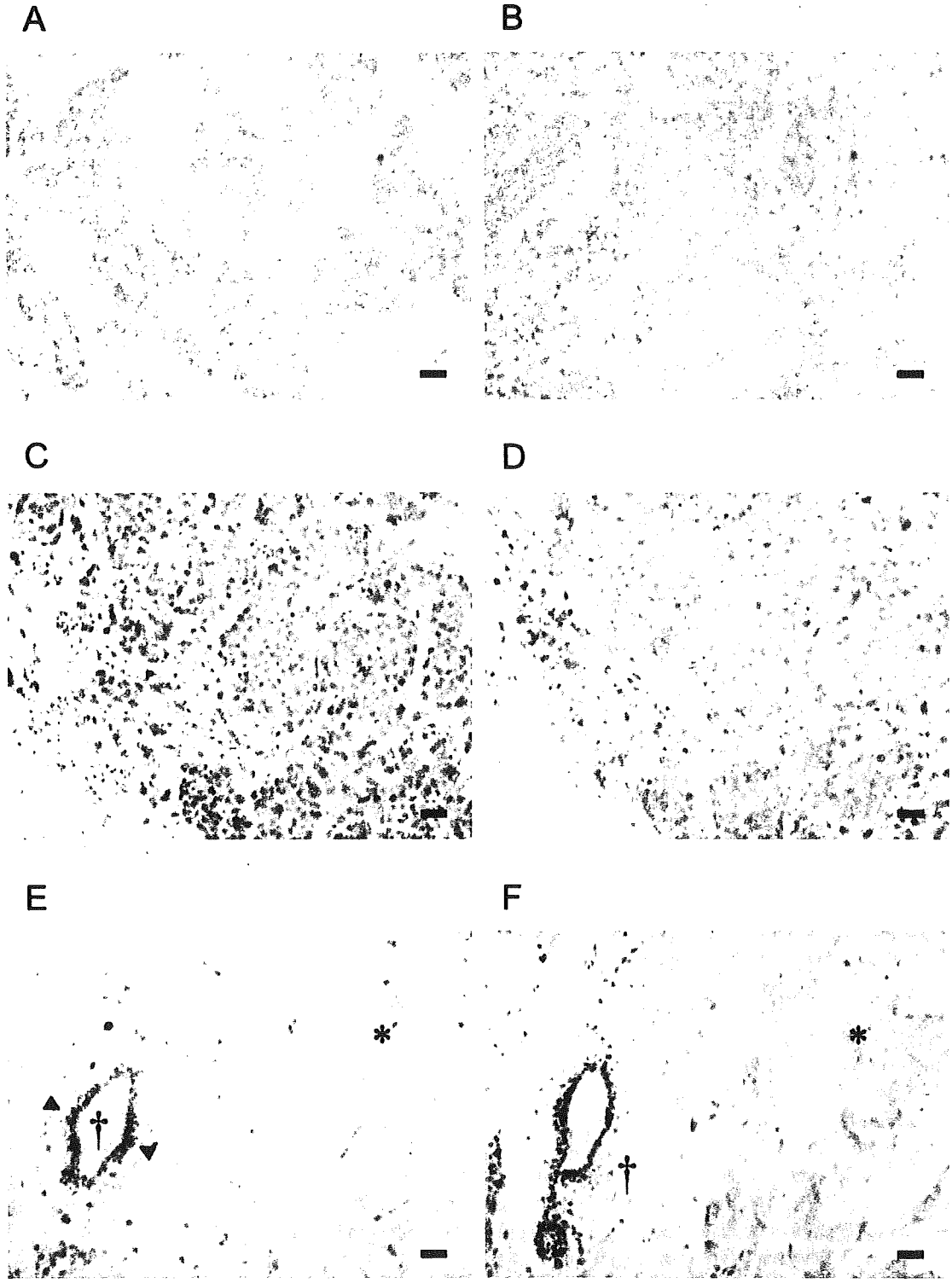

Figure 1. *Representative images of immunohistochemistry for TP and DPD in invasive ductal carcinoma of the breast. A, B: Negative cases of TP (A) and DPD (B) in breast carcinoma cases. There were no or low (<10%) TP or DPD immunoreactivities in breast carcinoma and intratumoral stromal cells, respectively. C, D: Positive cases of TP (C) and DPD (D) in breast carcinoma cases. There were high (<10%) immunoreactivities in breast carcinoma cells but not in intratumoral stromal cells. E, F: TP and DPD immunoreactivities in intratumoral stromal cells and in morphologically normal mammary glands. Immunoreactivity for TP (E) was partially detected in the cytoplasm of epithelial cells (†, arrow heads) but not stromal cells (*). Immunoreactivity for DPD (F) was detected in the cytoplasm of stromal cells (*) but not epithelial cells (†). Bar, 10 μm.*

breast tumor cells *in vitro* as a single agent by the following mechanisms: induction of apoptosis of breast carcinoma cells, as well as an inhibition of cell proliferation, as confirmed by TUNEL analyses. Several previous studies suggested that tumoral TP and DPD status could be considered as a good response factor in the carcinoma patients exposed to fluoropyrimidine drugs (17-19). In particular, TP expression in tumor tissue has been considered to clinically predict efficacy of capecitabine purely based on a theoretical background (10). However, this report is the first *in vitro* study evaluating the correlation between therapeutic efficacy of capecitabine and the levels of TP/DPD in breast carcinoma cells.

The results of our present study demonstrated that there were no correlations between the levels of *TP* and *DPD* mRNA levels and therapeutic efficacy of capecitabine in the treatment of BT-483 and MB-MDA-231 cells at all. These results suggest that at least in these two cells lines of human breast carcinoma, the status of the metabolizing enzymes TP and DPD in the carcinoma cells do not influence the therapeutic efficacy of capecitabine. It then becomes important to study the possible correlation between the enzyme levels of the carcinoma tissues and therapeutic efficacy of capecitabine in the specimens of neoadjuvant study. However, in our present study, the direct comparison between the status of these two enzymes and clinical response or efficacy of capecitabine could not be evaluated because the cases in which the specimens were available had not necessarily been administered capecitabine as a neoadjuvant treatment. In previously published studies of immunohistochemistry, TP was reported to be expressed at a significantly higher level in tumor tissue than in normal tissue of human breast (17, 18). Our findings of immunohistochemical study of TP in human breast cancer specimens (Figure 1A and 1B) were consistent with these results. In our present study, no statistically significant associations were detected between the status of TP and/or DPD immunoreactivity in carcinoma cells and intratumoral stromal cells and any of the clinicopathological factors of the patients examined. There was a statistically significant positive correlation between *TP* mRNA and protein levels in breast carcinoma tissues but none was detected for *DPD*. Takenoue *et al.* also reported a poor correlation between *DPD* mRNA and protein levels (20). The amount of DPD protein level in tumor and normal tissues was indeed very similar. These findings may explain the absence of any correlation between the results of immunohistochemical and RT-PCR studies of DPD because RT-PCR analysis in principle treated the tissues as a mass. Therefore, the presence of possible contamination or inclusion of non-neoplastic compartments in the specimens may have resulted in higher mRNA values of *DPD*. Oguri *et al.* also reported the absence of correlation between TP and the effects of 5-FU in non-small cell lung cancer (NSCLC) cell lines, although a significant positive correlation was reported in DPD status (21).

The lack of correlation between TP/DPD status and effects of capecitabine *in vitro* in cell lines and clinicopathological parameters in the patients also certainly cast reasonable doubts on the clinical significance of the intratumoral status of these two enzymes in breast carcinoma patients as potential surrogate markers of capecitabine treatment.

References

1 Pisani P, Parkin DM, Bray F and Ferlay J: Estimates of the worldwide mortality from 25 cancers in 1990. Int J Cancer *83*: 18-29, 1999.

2 Schüller J, Cassidy J, Dumont E, Roos B, Durston S, Banken L, Utoh M, Mori K, Weidekamm E and Reigner B: Preferential activation of capecitabine in tumor following oral administration to colorectal cancer patients. Cancer Chemother Pharmacol *45*: 291-297, 2000.

3 Liu G, Franssen E, Fitch MI and Warner E: Patient preferences for oral versus intravenous palliative chemotherapy. J Clin Oncol *15*: 110-115, 1997.

4 Homs MYV, Gaast A, Siersema PD, Steyerberg EW and Kuipers EJ: Chemotherapy for metastatic carcinoma of the esophagus and gastro-esophageal junction. Cochrane Database of Syst Rev *4*: CD004063, 2006.

5 Best L, Simmonds P, Baughan C, Buchanan R, Davis C, Fentiman I, George S, Gosney M, Northover J and Williams C: Colorectal Meta-analysis Collaboration. Palliative chemotherapy for advanced or metastatic colorectal cancer. BMJ *321*: 531-535, 2000.

6 Leonard RC: Oral fluoropyrimidines among the new drugs for patients with metastatic breast cancer. Br J Cancer *84*: 1437-1442, 2001.

7 Ranieri G, Grammatica L, Patruno R, Zito AF, Valerio P, Iacobellis S, Gadaleta C, Gasparini G and Ribatti D: A possible role of thymidine phosphorylase expression and 5-fluorouracil increased sensitivity in oropharyngeal cancer patients. J Cell Mol Med *11*: 362-368, 2007.

8 Walko CM and Lindley C: capecitabine: a review. Clin Ther *27*: 23-44, 2005.

9 Akiyama S, Furukawa T, Sumizawa T, Takebayashi Y, Nakajima Y, Shimaoka S and Haraguchi M: The role of thymidine phosphorylase, an angiogenic enzyme, in tumor progression. Cancer Sci *95*: 851-857, 2004.

10 Yonenaga F, Takasaki T, Ohi Y, Sagara Y, Akiba S, Yoshinaka H, Aikou T, Miyadera K, Akiyama S and Yoshida H: The expression of thymidine phosphorylase/platelet-derived endothelial cell growth factor is correlated to angiogenesis in breast cancer. Pathol Int *48*: 850-856, 1998.

11 Zhang X and Diasio BR: Regulation of human dihydropyrimidine dehydrogenase: implications in the pharmacogenetics of 5-FU-based chemotherapy. Pharmacogenomics *8*: 257-265, 2007.

12 Suzuki T, Nakata T, Miki Y, Kaneko C, Moriya T, Ishida T, Akinaga S, Hirakawa H, Kimura M and Sasano H: Estrogen sulfotransferase and steroid sulfatase in human breast carcinoma. Cancer Res *63*: 2762-2770, 2003.

13 Tokunaga Y, Sasaki H and Saito T: Clinical role of orotate phosphoribosyl transferase and dihydropyrimidine dehydrogenase in colorectal cancer treated with postoperative fluoropyrimidine. Surgery *141*: 346-353, 2007.

14 Loo WT, Sasano H and Chow LW: Evaluation of therapeutic efficacy of capecitabine on human breast carcinoma tissues and cell lines *in vitro*. Biomed Pharmacother *61*: 553-537, 2007.

15 Loo WT, Sasano H, Chow LW: Effects of capecitabine and vinorelbine on cell proliferation, metabolism and COX2 and p16 expression in breast cancer cell lines and solid tumour tissues. Biomed Pharmacother *61*: 596-600, 2007

16 Kim S and Taeuk Kim T: Selection of optimal internal controls for gene expression profiling of liver disease. BioTechniques *35*: 456-460, 2003.

17 Honda J, Sasa M, Moriya T, Bando Y, Hirose T, Takahashi M, Nagao T and Tangoku A: Thymidine phosphorylase and dihydropyrimidine dehydrogenase are predictive factors of therapeutic efficacy of capecitabine monotherapy for breast cancer preliminary results. J Med Invest *55*: 54-60, 2008.

18 Saeki T and Takashima S: Capecitabine plus docetaxel combination chemotherapy for metastatic breast cancer. Breast Cancer *11*: 116-120, 2004.

19 Ciccolini J, Evrard A and Cuq P: Thymidine phosphorylase and fluoropyrimidines efficacy: a Jekyll and Hyde story. Curr Med Chem Anticancer Agents *4*: 71-81, 2004.

20 Takenoue T, Kitayama J, Takei Y, Umetani N, Matsuda K, Nita ME, Hatano K, Tsuruo T and Nagawa H: Characterization of dihydropyrimidine dehydrogenase on immunohistochemistry in colon carcinoma, and correlation between immunohistochemical score and protein level or messenger RNA expression. Ann Oncol *11*: 273-279, 2000.

21 Oguri T, Achiwa H, Bessho Y, Muramatsu H, Maeda H, Niimi T, Sato S and Ueda R: The role of thymidylate synthase and dihydropyrimidine dehydrogenase in resistance to 5-fluorouracil in human lung cancer cells. Lung Cancer *49*: 345-351, 2005.

Received February 2, 2009
Revised May 8, 2009
Accepted May 13, 2009

Cancer Science
The official journal of the Japanese Cancer Association JCA

Steroid and xenobiotic receptor in human esophageal squamous cell carcinoma: A potent prognostic factor

Daisuke Takeyama,[1,2] Yasuhiro Miki,[1] Fumiyoshi Fujishima,[3] Takashi Suzuki,[1] Jun-ichi Akahira,[1] Shuko Hata,[1] Go Miyata,[2] Susumu Satomi[2] and Hironobu Sasano[1,3,4]

[1]Department of Pathology, [2]Division of Advanced Surgical Science and Technology, Tohoku University Graduate School of Medicine, Sendai, Miyagi; [3]Department of Pathology, Tohoku University Hospital, Sendai, Miyagi, Japan

(Received August 17, 2009/Revised September 17, 2009/Accepted September 23, 2009)

Steroid and xenobiotic receptor (SXR) is a nuclear receptor activated by diverse exogenous and endogenous compounds and has been demonstrated to play a pivotal role in detoxification through its regulation of various metabolizing enzymes and transporters. Recent studies also demonstrated the potential roles of SXR in the regulation of apoptosis and inflammation in various carcinoma cells, but the status of SXR in human esophageal squamous cell carcinoma (ESCC) has not been examined. Therefore, in this study, we performed immunohistochemical and quantitative RT-PCR evaluations in human ESCC in order to clarify its biological and clinical significance. We first immunolocalized SXR in 73 human ESCC cases. SXR immunoreactivity was detected in the nuclei, or in both nuclei and cytoplasm of carcinoma cells (98%, 20% of cases, respectively). The status of nuclear SXR immunoreactivity was inversely correlated with histological grade, lymph node status, ki67/MIB1 labeling index, and positively correlated with retinoid X receptor α status. In addition, high nuclear SXR expression was significantly correlated with favorable clinical outcome of the patients. Multivariate analysis further demonstrated SXR status in carcinoma cells as an independent favorable prognostic factor of the patients. Results of quantitative RT-PCR study demonstrated that SXR mRNA expression was detected in three of five cases, and was marked higher in the cancerous tissue than non-neoplastic tissue of these patients. This is the first study to demonstrate the status of SXR in human ESCC and the results suggest that SXR is a potent favorable prognostic factor of human ESCC. (*Cancer Sci* 2009)

Esophageal squamous cell carcinoma (ESCC) is one of the most lethal malignancies in some parts of the world including Japan, despite recent advances in therapeutic strategies including surgery, chemotherapy, radiotherapy, and combined therapies. Therefore, identifying and targeting factors associated with progression or chemotherapeutic efficacy of individual patients is required to improve the survival of ESCC patients.

Steroid and xenobiotic receptor (SXR; also called as human pregnane X receptor) is a member of the nuclear receptor superfamily of ligand-dependent transcription factors.[1,2] In humans, SXR is expressed mainly in the liver and small intestine, and plays a cardinal role in protecting tissues from potentially toxic exogenous and endogenous compounds. SXR is activated by structurally diverse ligands,[3,4] forms heterodimers with retinoid X receptor (RXR) α, and subsequently regulates transcription of its target genes.[5] Major target genes of SXR in human are drug-metabolizing enzymes and drug transporters such as cytochrome p450 (CYP) 3A4[1,2,6] and multidrug resistance gene 1 (MDR1).[7,8] CYP3A4 is a major phase I drug-metabolizing enzyme involved in the biotransformation of more than 50% of all known clinically used medications.[9] The *MDR1* gene encodes P-glycoprotein which is a member of ATP binding cassette transporter, and is considered to play an important role in developing the resistance of tumor cells to chemotherapy by exporting anticancer agents from intracellular to extracellular components.[10]

SXR has been reported to be expressed also in various human malignant tissue such as breast,[11–13] endometrial,[14] prostate,[15] and ovarian[16] cancer. Expression of SXR in carcinoma cells is usually associated with decreased sensitivity to anticancer drugs,[15–18] and drug–drug interactions.[19] In addition to these roles in metabolism, SXR has been also demonstrated to be involved in regulation of cell proliferation,[16] anti-apoptosis effect,[20] pro-apoptosis effect,[21,22] or inflammation.[23] Therefore, SXR has also been proposed to play a pivotal role in tumor progression in addition to these drug metabolism/efflux and drug–drug interactions described above.

In our previous study, SXR mRNA was not detected in the normal esophagus of the autopsy specimen.[24] However, a possible role of SXR in ESCC has not been examined. Therefore, in this study, we performed immunohistochemical study and quantitative RT-PCR in order to clarify the clinical or biological significance of SXR expression in patients with ESCC.

Materials and Methods

Patients and tissue preparation. Seventy-three specimens of thoracic ESCC were obtained from Japanese patients who underwent potentially curative esophagectomy with lymph node dissection from 1998 to 2003 at the Second Department of Surgery at Tohoku University Hospital (Sendai, Japan). These patients had not received any chemotherapy or irradiation prior to surgery. Sixteen specimens of non-neoplastic epithelium were obtained from these 73 cases. For immunohistochemistry, these specimens were fixed with 10% formalin and embedded in paraffin wax. Freshly frozen specimens were also available for RT-PCR analysis in some cases. Non-neoplastic esophageal mucosa and carcinoma tissues were obtained respectively from five ESCC patients who underwent esophagectomy in 2007 and these specimens were snap-frozen and stored at −80°C until examination. These five patients were all advanced cases. The depth of tumor invasion in these cases corresponded to either pT2 or pT3, and lymph node metastasis was detected in all five cases. No patients had received any chemotherapy or irradiation prior to surgery. Relevant clinical data were retrieved from careful review of the patient's charts. All tumors were reviewed by three of the authors (D.T., F.F., and H.S.). The pathological stage of each cancer was defined according to the TNM system

[4]To whom correspondence should be addressed.
E-mail: hsasano@patholo2.med.tohoku.ac.jp

doi: 10.1111/j.1349-7006.2009.01380.x

and each lesion was graded histologically according to the World Health Organization classification. The median follow-up time was 72 months (range, 2–133 months). The Ethics Committee at the Tohoku University School of Medicine approved the research protocols, and informed consent was obtained from each patient before surgery.

Antibodies. Mouse monoclonal antibody for SXR (PXR1) was kindly provided by Perseus Proteomics (Tokyo, Japan), and the antibody has been previously described in detail.[12] Verma *et al.* presented an immunoblotting analysis using the same monoclonal antibody and demonstrated its specificity.[22] Rabbit polyclonal antibody for RXRα was kindly provided by Professor Sugawara.[25] Other antibodies used in this study were as follows: mouse monoclonal antibodies for MDR1 (6C4.2), Ki-67 (MIB1), and p53 (DO-7) were purchased from Chemicon International (Temecula, CA, USA), Dako Cytomation (Kyoto, Japan), and Novocastra (Newcastle, UK), respectively. Rabbit polyclonal antibody for CYP3A4 was purchased from Chemicon.

Immunohistochemistry. Serial 3-μm thick tissue sections were deparaffinized with xylene and ethanol. Endogenous peroxidase activity was blocked by immersing the slides in 0.3% hydrogen peroxidase for 30 min at room temperature. Antigen retrieval was performed by heating the slides in an autoclave at 121°C for 5 min in citric acid buffer (2 mmol/L citric acid and 9 mmol/L trisodium citrate dehydrate, pH6.0) or instant antigen retrieval H buffer (Mitsubishi Kagaku Iatron, Tokyo, Japan). Sections were then incubated with 10% normal rabbit serum for the monoclonal antibodies, or normal goat serum for polyclonal antibody to reduce nonspecific background immunostaining. The reacted sections were then incubated for 16 h at 4°C with primary antibodies. The dilutions of primary antibodies were as follows: SXR, 1:400; RXRα, 1:3500; CYP3A4, 1:1000; MDR1, 1:40; Ki-67, 1:100; and p53, 1:200. The sections were subsequently incubated with biotinylated rabbit antimouse IgG or goat antirabbit IgG (Histofine Kit; Nichirei, Tokyo, Japan), and with horseradish peroxidase–conjugated streptoavidin (Nichirei). The antigen–antibody complex was then visualized with 3.3′-diaminobenzidine (1 mmol/L, in 50 mol/L Tris–HCl buffer, pH 7.6, and 0.006% H_2O_2) and counterstained with hematoxylin. Normal small intestine was used as a positive control for SXR. As a negative control, normal mouse or rabbit IgG was used instead of the primary antibodies and no specific immunoreactivity was detected.

Immunohistochemical analysis. Immunoreactivity for SXR was detected in the nuclei or in the nuclei and cytoplasm. For semiquantitative analysis of nuclear SXR immunoreactivity, the H score was used in this study.[26] Briefly, more than 1000 tumor cells were counted in three different representative areas corresponding to the invasive front of the tumor in each case, and the H score was derived from the formula: H score = (percentage of strongly stained nuclei × 3) + (percentage of moderately stained nuclei × 2) + (percentage of weakly stained nuclei × 1). This formula gives a possible range of 0–300. The staining intensity of SXR in the cytoplasm was classified in two categories: negative or positive. Immunoreactivity for RXRα, Ki67, and p53 were detected in the nuclei. These immunoreactivities were evaluated in more than 1000 carcinoma cells in each case, and were counted, and the percentage of immunoreactivity (i.e. labeling index [LI]) was determined. Scoring was done independently by two of the authors (D.T. and F.F.). Interobserver differences were less than 5%, and the mean of the value was obtained as a final value of LI. For p53 immunohistochemistry, cases with an LI of more than 10% were determined to be positive according to the results of previous report.[27]

For analysis evaluating the possible correlation between SXR status and clinical outcome of individual patients, the cases were classified into two groups according to SXR H score (high SXR, >100 H score; low SXR, 0–99 H score), because SXR H scores were distributed in two peaks on the boundary of approximately 100. In addition, the median value of the SXR H score was 98.1, near the value of 100. The selection of the median value as the cut-off point is usually considered to secure objectivity because it is not determined as an "optimal" cut-off point.[28]

Real-time RT-PCR. Total RNA was carefully extracted from the specimens of carcinoma and non-neoplastic tissues from five ESCC patients and two human ESCC cell lines (TE10, obtained from the Cell Resource Center for Biomedical Research, Institute of Development, Aging and Cancer, Tohoku University, Sendai, Japan; EC-GI-10, obtained from RIKEN BioResource Center, Ibaraki, Japan) using the TRIzol (Invitrogen Life Technologies, Gaithersburg, ND) method. The QuantiTect Reverse Transcription kit (Qiagen, Hilden, Germany) was employed in the synthesis of cDNA. Real-time PCR was carried out using the LightCycler System and FastStat DNA Master SYBR Green I (Roche Diagnostics, Mannheim, Germany). The PCR primer sequences for SXR and PRL13A used in this analysis were as follows: SXR, forward 5′-CCCAGTGTCAACGCAGATGAG-3′, reverse 5′-GTTGCGTTTCATGGCCCTC-3′; RPL13A, forward 5′- CCTGGAGGAGAAGAGGAAAGAGA-3′, reverse 5′-TTGAGGACCTCTGTGTATTTGTCAA-3′. An initial denaturing step of 95°C for 10 min was followed by 40 cycles for SXR, 35 cycles for PRL13A at 95°C for 10 s; 15 s annealing at 75°C (SXR), 68°C (PRL13A); and extension for 15 s at 72°C. RNA from cultured human liver cells (HuH7; human hepatocellular carcinoma obtained from the Cell Resource Center for Biomedical Research) were used as a positive control for SXR. Negative controls, in which the reaction mixture lacked cDNA template, were included to check for the possibility of exogenous contaminant DNA. cDNA of known concentration for SXR and the housekeeping gene *RPL13A* was used generate standard curves for real-time quantitative PCR in order to determine the quantity of target cDNA transcripts. The mRNA level in each case was represented as a ratio of RPL13A and was evaluated as a ratio (%) compared with that of positive control.[12,29]

Statistical analysis. Values for SXR H score, patient age, tumor size, Ki67/MIB1 LI, and RXRα LI were demonstrated as mean ± SEM. The statistical analyses between SXR H score and clinicopathological parameters were evaluated using the Mann–Whitney *U*-test, Kruskal–Wallis test, a correlation coefficient (r), and regression equation when appropriate. The statistical analyses between the status of cytoplasmic SXR immunoreactivity and clinicopathological parameters were evaluated using the χ^2-test or Mann–Whitney *U*-test when appropriate. Overall survival (OS) and disease-free survival (DFS) curves of the patients examined were generated according to the Kaplan–Meier method and statistical significance was calculated using the log-rank test. Cox's proportional hazard model was used for both univariate and multivariate analyses. Statistical differences were examined using StatView 5.0 J software (SAS Institute, Cary, NC, USA) and values of $P < 0.05$ were considered statistically significant.

Results

Immunohistochemical staining. SXR immunoreactivity was detected in the nuclei in non-neoplastic epithelial cells of the esophagus (Fig. 1a). Immunoreactivity was abundant in the suprabasal layer (mean H score = 67.2 ± 3.2) compared with the basal layer (mean H score = 28.4 ± 3.1). SXR immunoreactivity in non-neoplastic epithelial cells was relatively low compared to that in carcinoma cells. In 72 out of 73 cases, SXR immunoreactivity was detected in the nuclei of carcinoma cells with a variety of the immunointensity (Fig. 1b–d). The mean value of the SXR H score in 73 ESCC was 94.6 ± 5.1 (range, 0–211). In only one case, SXR immunoreactivity was not detected in both nuclei and

doi: 10.1111/j.1349-7006.2009.01380.x

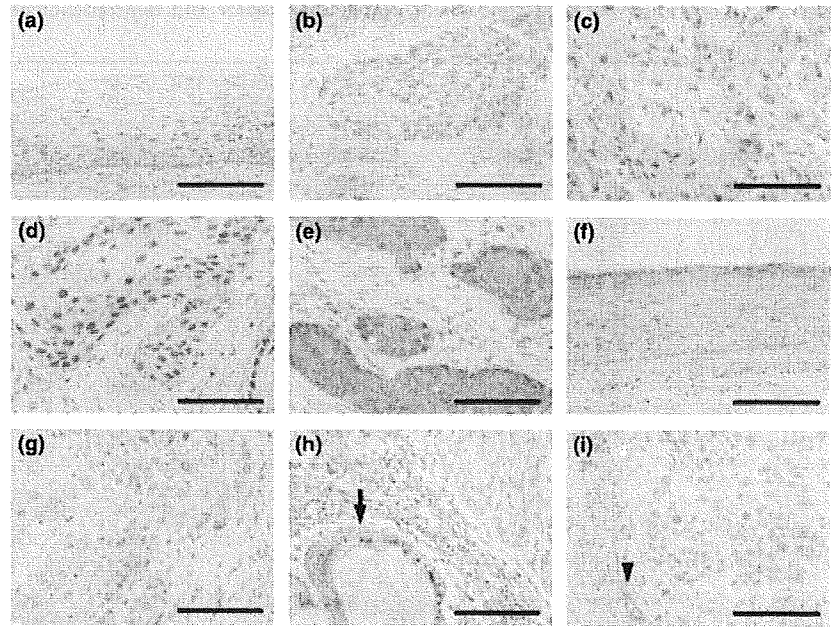

Fig. 1. Representative illustrations of immunohistochemistry in human esophageal squamous cell carcinoma. (a) Immunoreactivity for steroid and xenobiotic receptor (SXR) was detected in the nuclei of non-neoplastic epithelial cells. (b–d) Immunoreactivity for SXR was detected in the nuclei of carcinoma cells. (b) Weakly, (c) moderately, and (d) strongly stained patterns of SXR immunoreactivity. (e) Immunoreactivity for SXR was detected in both the nuclei and cytoplasm of the carcinoma cells. (f) Immunoreactivity for retinoid X receptor α was detected in the nuclei of non-neoplastic esophageal epithelial cells (g) and carcinoma cells. (h) Immunoreactivity for cytochrome p450 3A4 was detected in esophageal glands (arrow), but not in carcinoma cells. (i) Immunoreactivity for MDR1 was detected in capillary vessels (arrow head), but not in carcinoma cells. Bar, 100 μm.

cytoplasm, but no clinicopathological characteristics specific to this particular case were identified. In 15 out of 73 cases examined, SXR immunoreactivity was detected in both the nuclei and cytoplasm of carcinoma cells (Fig. 1e). There was no significant association between SXR immunmoreactivity in the nucleus and cytoplasm. The mean SXR H score was 76.9 ± 5.6 in cytoplasmic SXR positive cases, and 98.4 ± 11.3 in cytoplasmic SXR negative cases ($P = 0.1405$). RXRα immunoreactivity was detected in the nuclei of non-neoplastic epithelial cells and carcinoma cells (Fig. 1f,g). CYP3A4 and MDR1 immunoreactivity was not detected in carcinoma cells, although CYP3A4 immunoreactivity was detected only in esophageal glands, and MDR1 in some capillary vessels (Fig. 1h,i).

Correlation between the status of SXR immunoreactivity and clinicopathological variables in 73 ESCC patients. Associations between SXR status and clinicopathological variables of the patients examined are summarized in Table 1. There was a significant inverse association between the SXR H score and tumor differentiation ($P = 0.0301$), but cytoplasmic SXR immunoreactivity was positively associated with tumor differentiation ($P = 0.0032$). There was an inverse significant association between the SXR H score and presence of lymph node metastasis ($P = 0.0199$). There was a positive significant correlation between the SXR H score and RXRα LI ($P = 0.0009$, $r = 0.382$). Ki67/MIB1 LI was inversely correlated with the SXR H score ($P = 0.0419$, $r = -0.238$), but was positively correlated with the status of cytoplasmic SXR immunoreactivity ($P = 0.0049$). No significant association was detected between SXR immunoreactivity and age, gender, tumor size, TNM stage, lymphatic invasion, or venous invasion, and the p53 status of the patients examined.

Correlation between SXR status and clinical outcome in the 73 ESCC patients. OS and DFS curves of the patients examined are illustrated in Figure 2. The statistical analysis demonstrated that high nuclear SXR expression in ESCC patients was significantly associated with better survival or favorable clinical outcome of the patients examined in this study (log-rank test: OS, $P = 0.0026$; DFS, $P = 0.0027$). Significant correlation was not detected between SXR status in the cytoplasm and prognosis of the patients. The results of univariate analysis (Tables 2 and 3) demonstrated that pathological stage (OS, $P = 0.0002$; DFS, $P < 0.0001$), SXR status in the nucleus of carcinoma cells (OS, $P = 0.0041$; DFS, $P = 0.0045$), presence of venous invasion (OS, $P = 0.0139$; DFS, $P = 0.0239$), tumor size (OS, $P = 0.0294$; DFS, $P = 0.0078$), gender (OS, $P = 0.0392$; DFS, $P = 0.0270$), presence of lymphatic invasion (OS, $P = 0.0465$), and RXRα status (DFS, $P = 0.0332$) all turned out to be significant prognostic factors for OS and/or DFS in the 73 ESCC patients examined. A subsequent multivariate analysis, however, demonstrated that only SXR status in the nucleus (OS, $P = 0.0151$; DFS, $P = 0.0252$) was an independent prognostic factor for OS and DFS, as well as pathological stage (OS, $P = 0.0042$; DFS, $P = 0.0052$) and tumor size (OS, $P = 0.0414$; DFS, $P = 0.0106$).

Quantitative RT-PCR analysis. The results of quantitative RT-PCR of SXR are summarized in Figure 3. SXR mRNA expression was detected in three of five carcinoma tissues of ESCC patients examined in this study. SXR mRNA levels ranged from 0% to 10% of the positive controls with an average ± SD of 3.89 ± 5.17%. In two carcinoma tissues in which SXR mRNA was below the detection limit, PCR products for SXR appeared as a faint but definitive band in gel electrophoresis. In non-neoplastic mucosa, SXR mRNA expression was detected in three of five cases and SXR mRNA levels ranged from 0% to 0.13% with an average ± SD of 0.03 ± 0.05%. No correlation was identified between SXR mRNA level and the clinicopathological variables of the patients examined. In three cases in which SXR mRNA was detected in carcinoma tissues, SXR immunoreactivity tended to be higher than the two cases in which SXR mRNA was not detected. In non-neoplastic epithelium of these five cases, SXR immunoreactivity was detected in a similar fashion. SXR mRNA expression in non-neoplastic mucosa was marked low compared to the level of cancerous tissue. SXR mRNA was not detected in two human ESCC cell lines examined in this study.

Discussion

To the best of our knowledge, this is the first study to demonstrate expression of SXR in ESCC. We previously reported that SXR mRNA was not detected in an esophagus obtained from autopsy,[24] but only one autopsy specimen was examined by RT-PCR in this reported analysis. In our present study, we demonstrated the expression of both SXR protein and SXR mRNA

Table 1. Correlation between steroid and xenobiotic receptor and clinicopathological variables in 73 esophageal squamous cell carcinoma patients

Variable	*n* or mean ± SEM (range)	Nuclear SXR		Cytoplasmic SXR		
		H score (mean ± SEM)	*P*-values	Negative (*n* = 58)	Positive (*n* = 15)	*P*-values
				n (%)	*n* (%)	
Age (years)						
<65	36	95.4 ± 7.8	0.9084	27 (75.0)	9 (25.0)	0.3975
≥65	37	93.7 ± 6.8		31 (83.8)	6 (16.2)	
Gender						
Men	61	91.1 ± 5.3	0.2005	47 (77.0)	14 (23.0)	0.4385
Women	12	112.1 ± 14.9		11 (91.7)	1 (8.3)	
Tumor size (mm)						
<50	39	90.1 ± 7.5	0.4324	31 (79.5)	8 (20.5)	>0.9999
≥50	34	99.6 ± 6.7		27 (79.4)	7 (20.6)	
TNM-pT						
pT1	34	96.9 ± 8.4	0.5481	28 (82.4)	6 (17.6)	0.8163
pT2	10	100.0 ± 15.9		8 (80.0)	2 (20.0)	
pT3	29	89.9 ± 6.4		22 (75.8)	7 (24.2)	
TNM-pN						
pN0	33	107.1 ± 8.3	**0.0199**	27 (81.8)	6 (18.2)	0.6495
pN1	40	84.2 ± 5.9		31 (77.5)	9 (22.5)	
TNM-pM						
pM0	67	95.5 ± 5.4	0.4947	55 (82.1)	12 (17.9)	0.0968
pM1(LYM)	6	83.7 ± 15.6		3 (50.0)	3 (50.0)	
TNM-pStage						
I	24	104.6 ± 10.3	0.5394	19 (79.2)	5 (20.8)	0.2271
II	25	91.2 ± 9.3		22 (88.0)	3 (12.0)	
III	18	89.3 ± 7.2		14 (77.8)	4 (22.2)	
IV	6	83.7 ± 15.6		3 (50.0)	3 (50.0)	
Differentiation						
Well	13	109.5 ± 10.3	**0.0301**	12 (92.3)	1 (7.7)	**0.0032**
Moderately	50	96.9 ± 6.1		42 (84.0)	8 (16.0)	
Poorly	10	63.5 ± 12.9		4 (40.0)	6 (60.0)	
Lymphatic invasion						
Negative	30	92.5 ± 8.8	0.9196	24 (80.0)	6 (20.0)	0.9229
Positive	43	96.0 ± 6.2		34 (79.1)	9 (20.9)	
Venous invasion						
Negative	33	97.5 ± 8.6	0.6336	27 (81.8)	6 (18.1)	0.6495
Positive	40	92.2 ± 6.2		31 (77.5)	9 (22.5)	
RXRα LI (%)	36.5 ± 2.2 (0–76.2)		**0.0009** (r = 0.382)	37.3 ± 2.5 (0–76.2)	33.2 ± 4.9 (0–65.8)	0.4834
Ki67/MIB1 LI (%)	40.7 ± 1.4 (19.1–69.6)		**0.0419** (r = −0.238)	38.6 ± 1.3 (19.1–69.6)	48.8 ± 3.6 (22.9–69.3)	**0.0049**
p53 immunoreactivity						
Negative	25	108.0 ± 8.7	0.0663	21 (84.0)	4 (16.0)	0.4877
Positive	48	87.5 ± 6.2		37 (77.1)	11 (22.9)	

Data are presented as mean ± SEM. All other values represent the number of cases. *P*-values less than 0.05 were considerd significant, and are shown in bold. LI, labeling index; RXR, retinoid X receptor; SXR, steroid and xenobiotic receptor.

in the non-neoplastic esophagus as well as in ESCC. Results of our present study demonstrated that the expression of SXR protein and mRNA was markedly higher in carcinoma tissue compared with non-neoplastic esophagus. SXR was not detected in normal tissue of the breast[12] and endometrium,[14] and SXR was weakly expressed in normal prostate tissue compared with cancerous tissue.[15] Results from our present study and previous studies above all suggest that SXR was more abundantly expressed in carcinoma cells than in their normal counterparts. SXR immunoreactivity in the nuclei was detected in almost all cases, although in some cases SXR immunoreactivity was detected in both the nuclei and cytoplasm of the carcinoma cells in ESCC. SXR is localized in the cytoplasm of mouse liver and is translocated into the nucleus following administration of its ligands.[30] In addition, SXR forms a heterodimer with RXRα upon binding to specific repeats in the promoter regions of its target genes.[5] In our present study, SXR immunoreactivity in the nucleus was positively correlated with RXRα immunoreactivity. Therefore, SXR expression in the nucleus is considered to play a more functional role than cytoplasmic SXR expression. In our present study, *CYP3A4* and *MDR1*, which are both well-known target genes regulated by SXR in the liver or other tissues, were not detected at all in ESCC cells. Therefore, SXR is considered to regulate some other drug-metabolizing enzyme or transporter genes in the esophagus. However, SXR may also contribute to cancer progression or development through regulating genes other than drug-metabolizing enzymes or transporters in ESCC cells. Further investigations are required to identify the potential target genes of SXR in ESCC.

The SXR H score in carcinoma cells was inversely correlated with the presence of lymph node metastasis, and subsequent prognostic analysis revealed that a relatively high nuclear SXR

doi: 10.1111/j.1349-7006.2009.01380.x

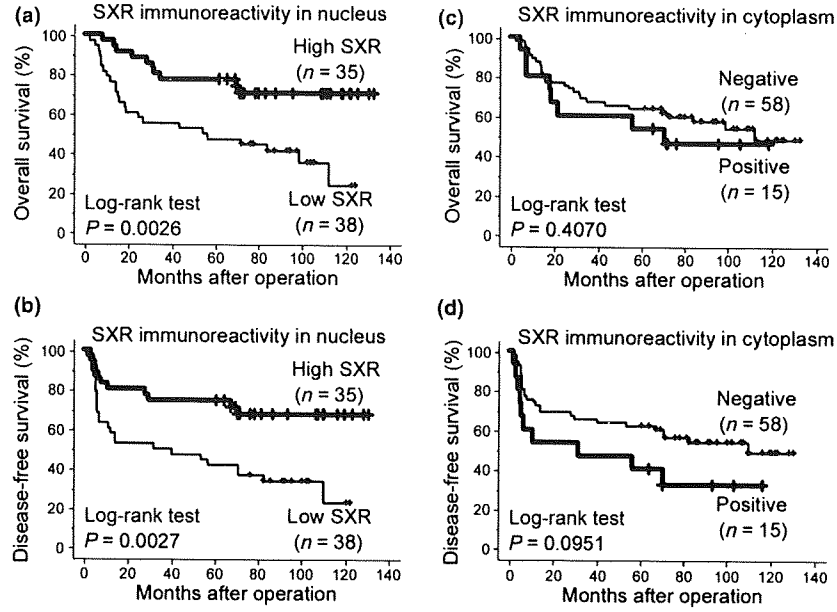

Fig. 2. Overall and disease-free survival (OS and DFS) curves of 73 patients with esophageal squamous cell carcinoma examined in this study according to the status of steroid and xenobiotic receptor (SXR) immunoreactivity (Kaplan–Meier method). Significant difference in survival of the patients was detected between patients with high and low SXR nuclear expression (a,b), but significant difference was not detected according to the status of SXR cytoplasmic expression (c,d). Cases were classified into two groups according to SXR H score in the nucleus: high SXR, >100 H score; low SXR, 0–99 H score. High SXR status was significantly associated with favorable clinical outcome.

Table 2. Univariate and multivariate analysis of overall survival in 73 esophageal squamous cell carcinoma patients

Variable	Univarate		Multivariate	
	P-values	Relative risk (95% CI)	*P*-values	Relative risk (95% CI)
Gender (men/women)	**0.0392**	4.537 (1.078–19.097)	0.2931	2.189 (0.508–9.428)
Age, years (≥65/<64)	0.2147	1.545 (0.777–3.071)		
Tumor size (≥50 mm/<49 mm)	**0.0294**	2.152 (1.079–4.290)	**0.0414**	2.346 (1.034–5.326)
Histological grade (poor/well, moderate)	0.8627	1.087 (0.421–2.812)		
Lymphatic invasion (positive/negative)	**0.0465**	2.131 (1.012–4.439)	0.8131	1.108 (0.473–2.599)
Venous invasion (positive/negative)	**0.0139**	2.556 (1.210–5.400)	0.5381	1.302 (0.562–3.016)
TNM-pStage (III, IV/I, II)	**0.0002**	4.039 (1.934–8.435)	**0.0042**	3.298 (1.457–7.464)
Nuclear SXR status (low/high)	**0.0041**	2.956 (1.409–6.203)	**0.0151**	2.817 (1.222–6.495)
p53 status (positive/negative)	0.7997	0.913 (0.451–1.847)		
Ki67 status†	0.5376	1.009 (0.981–1.038)		
RXRα status†	0.0546	0.983 (0.967–1.000)		

†Data were evaluated as continuous values. Data considered significant ($P < 0.05$) in the univariate analysis are shown in bold and were examined in the multivariate analysis. CI, confidence interval; RXR, retinoid X receptor; SXR, steroid and xenobiotic receptor.

Table 3. Univariate and multivariate analysis of disease-free survival in 73 esophageal squamous cell carcinoma patients

Variable	Univarate		Multivariate	
	P-values	Relative risk (95% CI)	*P*-values	Relative risk (95% CI)
Gender (men/women)	**0.0270**	5.027 (1.201–21.040)	0.0939	3.416 (0.811–14.381)
Age, years (≥65/<64)	0.3652	1.353 (0.703–2.600)		
Tumor size (≥50 mm/<49 mm)	**0.0078**	2.397 (1.235–4.652)	**0.0106**	2.512 (1.239–5.091)
Histological grade (poor/well, moderate)	0.1414	1.855 (0.814–4.230)		
Lymphatic invasion (positive/negative)	0.1667	1.563 (0.794–3.077)		
Venous invasion (positive/negative)	**0.0239**	2.231 (1.112–4.475)	0.1602	1.716 (0.808–3.646)
TNM-pStage (III, IV/I, II)	**<0.0001**	4.331 (2.206–8.503)	**0.0052**	2.891 (1372–6.091)
Nuclear SXR status (low/high)	**0.0045**	2.792 (1.374–5.671)	**0.0252**	2.371 (1.113–5.050)
p53 status (positive/negative)	0.7406	1.123 (0.564–2.237)		
Ki67 status†	0.4878	1.010 (0.982–1.040)		
RXRα status†	**0.0332**	0.982 (0.966–0.999)	0.5582	0.994 (0.976–1.013)

†Data were evaluated as continuous values. Data considered significant ($P < 0.05$) in the univariate analysis are shown in bold and were examined in the multivariate analysis. CI, confidence interval; RXR, retinoid X receptor; SXR, steroid and xenobiotic receptor.

expression of ESCC cells was significantly associated with favorable clinical outcome and was an independent favorable prognostic factor in this group of ESCC patients examined. These findings are in disagreement with the previous report by Conde that high SXR expression is a poor prognostic factor in breast cancer.[13] Conde *et al.* reported that SXR expression was

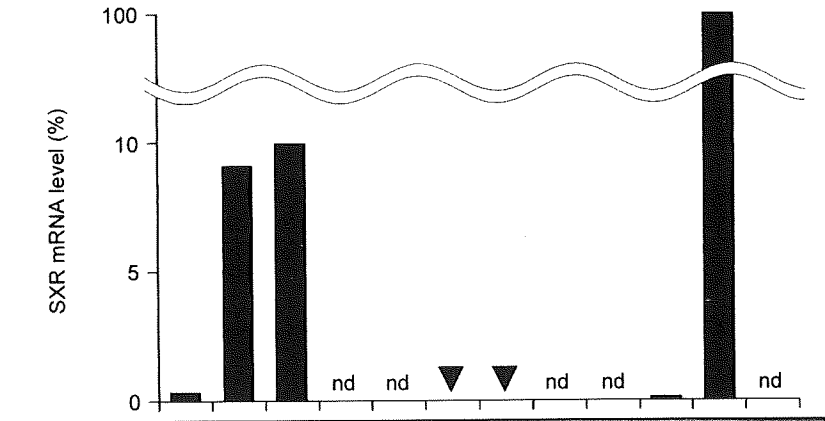

Case	Carcinoma tissue #1	#2	#3	#4	#5	Non-neoplastic mucosa #1	#2	#3	#4	#5
SXR H-score	90.1	100.4	87.1	41.3	37.0	30.9	47.5	44.0	65.5	54.7
SXR cytoplasm	+	–	–	+	–	–	–	–	–	–

Fig. 3. Result of quantitative RT-PCR for steroid and xenobiotic receptor (SXR) of carcinoma and non-neoplastic esophageal mucosa in esophageal squamous cell carcinoma cases. SXR mRNA was detected in three out of five cases in carcinoma tissue (cases #1, #2, #3) and non-neoplastic esophageal mucosa (cases #1, #2, #5), respectively. Cases #4 and #5 were associated with a faint but definitive band in carcinoma tissues, although in quantitative PCR SXR mRNA was below the detection limit (SXR, 0.001 pg/μL). The expression level in non-neoplastic mucosa was very low compared with that of carcinoma tissue. SXR mRNA level is represented as a ratio of housekeeping gene the ribosomal protein L13A (*RPL13A*), and was evaluated as ratio (%) compared with that of positive control. arrowhead, 0.01%; M, marker; NC, negative control; nd, undetectable level; PC, positive control.

inversely correlated with estrogen receptor, and the SXR pathway may contribute to potential poor response to the endocrine adjuvant therapy. *In vitro*, some studies, however, demonstrated that SXR activation is involved in the processes of anti-apoptotic [20,31] and proliferative effects to the carcinoma cells.[16,32] In contrast, Verma *et al.* reported a pro-apoptotic effect of SXR activation in breast cancer cells in conjunction with wild-type p53.[22] They demonstrated that SXR activation by xenobiotic ligands resulted in the up-regulation of inducible nitric oxicide synthase (iNOS) and calmodulin, which subsequently caused local production of nitric oxide (NO) and NO-dependent up-regulation of p53, with eventual cell arrest or apoptosis of carcinoma cells. These discrepancies in SXR functions between an anti-apoptotic effect in some tissues and a pro-apoptotic effect in others may be due to its tissue-specific or ligand-promoter-dependent manner.[33,34] SXR was reported to regulate *iNOS* gene expression through the DR4-mediated activation of human iNOS promoter activity,[35] and iNOS was expressed abundantly in carcinoma cells of human ESCC.[36,37] In our present study, the p53-negative group tended to be associated with higher SXR H score but this association did not reach statistical significance. This may be due to the fact that the p53 phenotype was not necessarily correlated with the p53 genotype,[38] and the apoptosis pathway through p53 is known to be very complicated.[39] In addition, NO is well known to process cytostatic effects through directly influencing the levels of cyclin D1, independent of the p53 pathway.[40] Therefore, the SXR–iNOS–NO pathway may be involved in the pro-apoptotic effect in ESCC cells, independently of p53 status.

Nuclear factor-kappa B (NF-κB) is also one of transcription factors involved in regulation of inflammation and immune responses. Activation of NF-κB results in an elevated expression of cell cycle genes, inhibitor of apoptosis, and protease which subsequently promote the process of invasion of carcinoma cells, and play an important role in malignant behavior.[41] Recently, mutual repression between SXR and NF-κB was also reported.[23] These results suggest that an activation of SXR inhibits the activity of NF-κB, which may result in inhibition of cell proliferation, anti-apoptosis, invasive property, and angiogenesis. Therefore, results of these *in vitro* studies and our present study suggest that high nuclear SXR expression may contribute to the lower proliferative activity of carcinoma cells, diminished invasive and metastatic potentials, and favorable clinical outcome of the patients.

In our present study, positive SXR immunoreactivity in the cytoplasm tended to be associated with a poor prognosis, but this association did not reach statistical significance. The opposite correlation between nuclear and cytoplasmic SXR status in this study suggests that SXR may be translocated into the nucleus from the cytoplasm *in vitro*. Another possible explanation is the nongenomic action of nuclear receptor. For example, estrogen receptor can mediate signaling cascades at the membrane and in the cytoplasm via various second messengers, such as receptor-mediated protein kinases.[42] In lung cancer cells, the proliferative effects of estrogen were mediated primarily by the nongenomic action of ERβ.[43] In addition, Conde *et al.* reported that cytoplsmic localization of SXR represented poor prognosis as well as nuclear localization of SXR.[13] Nongenomic action has not been reported in SXR mediated actions, to the best of our knowledge, but nongenomic action with extranuclear SXR may play important roles in modulating the proliferation of esophageal cancer cells. However, further investigations are required to clarify the possible role of SXR in the biological behavior of ESCC.

In summary, we demonstrated expression of SXR using immunohistochemistry and quantitative RT-PCR in human

doi: 10.1111/j.1349-7006.2009.01380.x